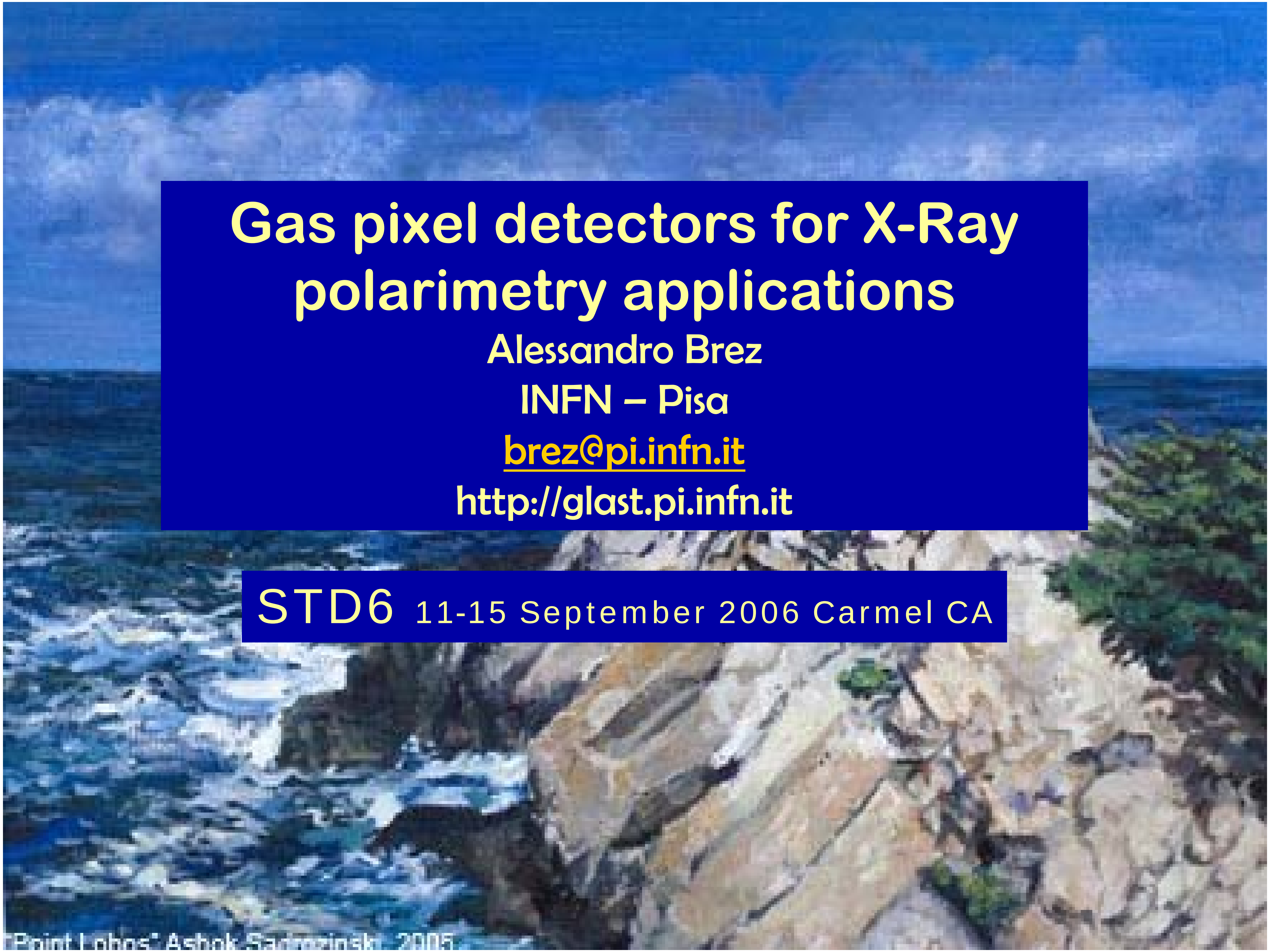

# Gas pixel detectors for X-Ray polarimetry applications


Alessandro Brez

INFN – Pisa

brez@pi.infn.it

http://glast.pi.infn.it


STD6 11-15 September 2006 Carmel CA

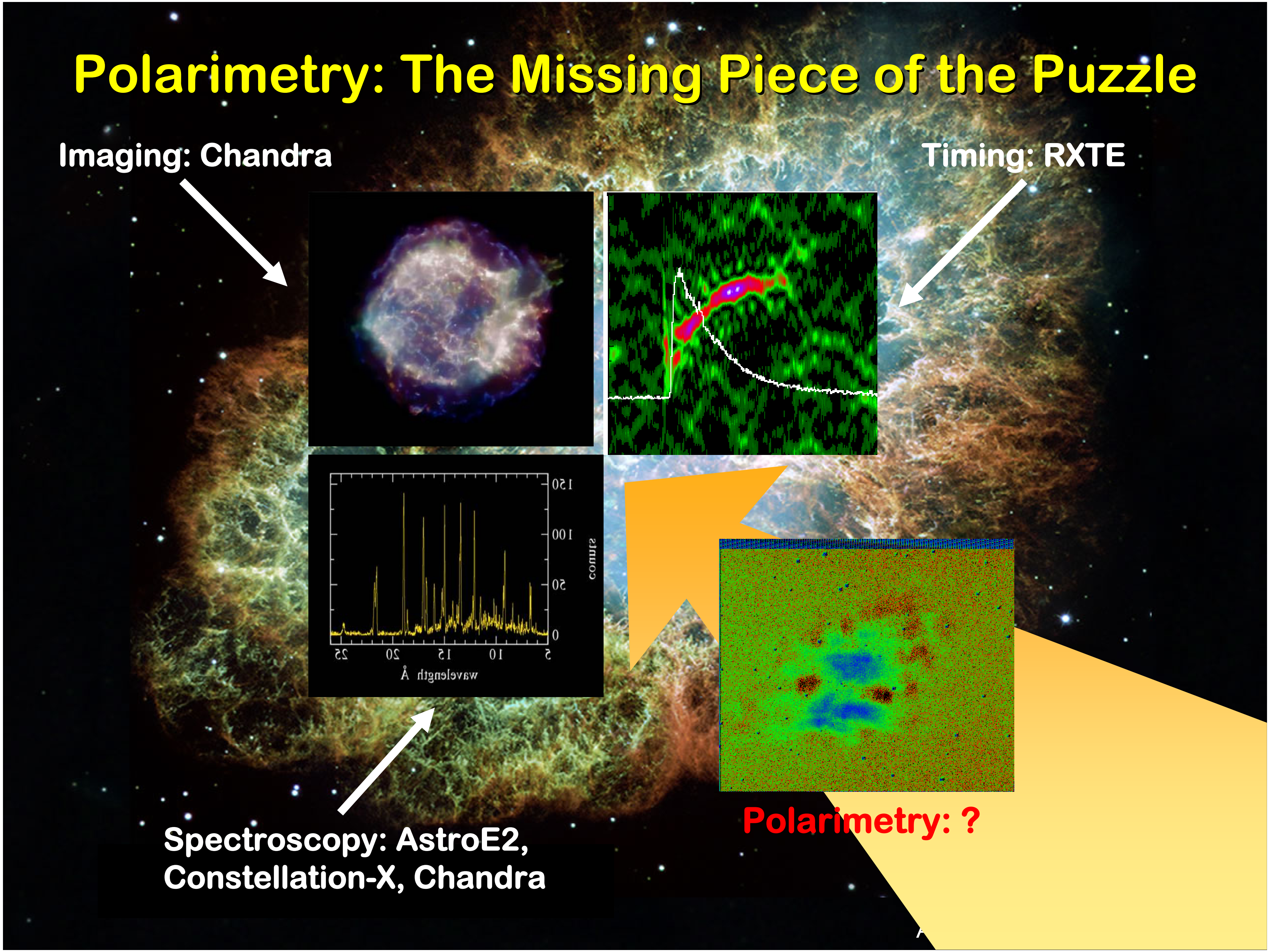
Polarimetry: The Missing Piece of the Puzzle
Imaging: Chandra
Timing: RXTE
Spectroscopy: AstroE2,
Constellation-X, Chandra
Polarimetry: ?

# Photoelectric cross section

**The photoelectric effect is very sensitive to photon polarization!**

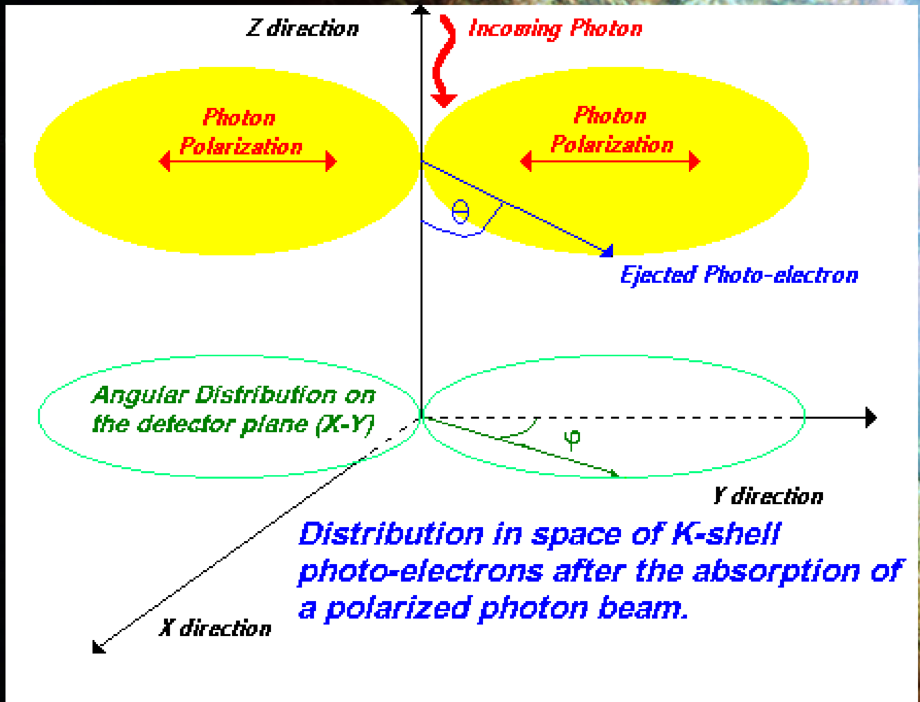


Simple analytical expression for photoemission differential cross section (k-shell photoelectron in non-relativistic limit):

$$\frac{\partial\sigma}{\partial\Omega} = r_o^2 \frac{Z^5}{137^4}\left(\frac{mc^2}{h\nu}\right)^{7/2} \frac{4\sqrt{2}\sin^2(\theta)\cos^2(\varphi)}{(1-\beta\cos(\theta))^4}$$

If we project on the plane orthogonal to the propagation direction…

$$\frac{\partial\sigma}{\partial\Omega} \propto \cos^2\phi$$

# Photoelectron and Auger angular distributions

## Photoelectron emission angular distributions

$$\frac{\partial\sigma}{\partial\theta} \propto \frac{\sin^3(\theta)}{(1-\beta\cos(\theta))^4}$$

$$\frac{\partial\sigma}{\partial\phi} \propto \cos^2\phi$$

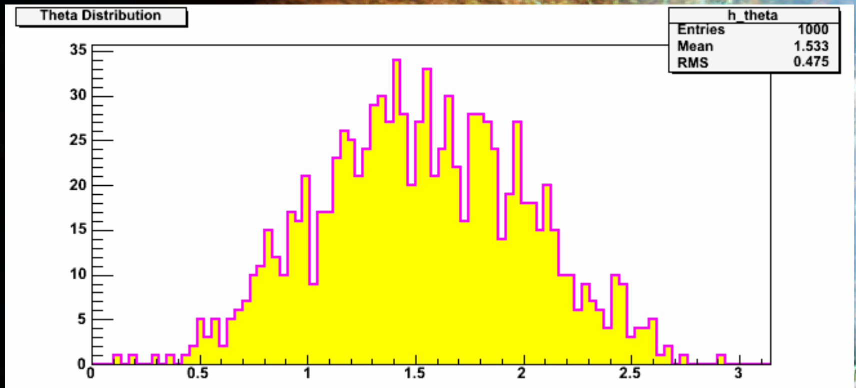


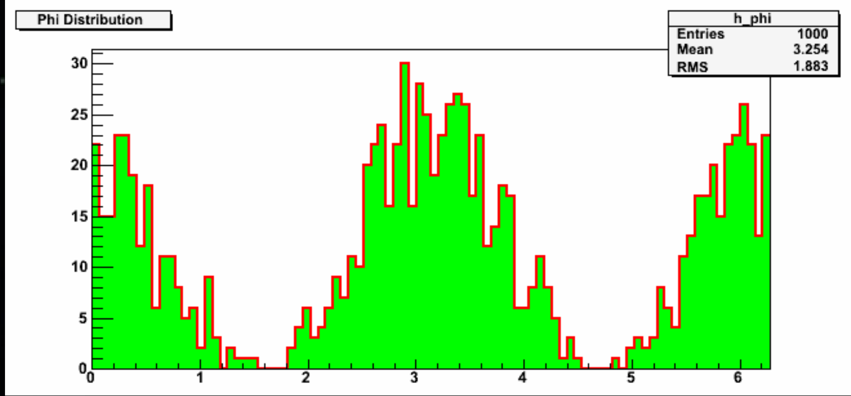


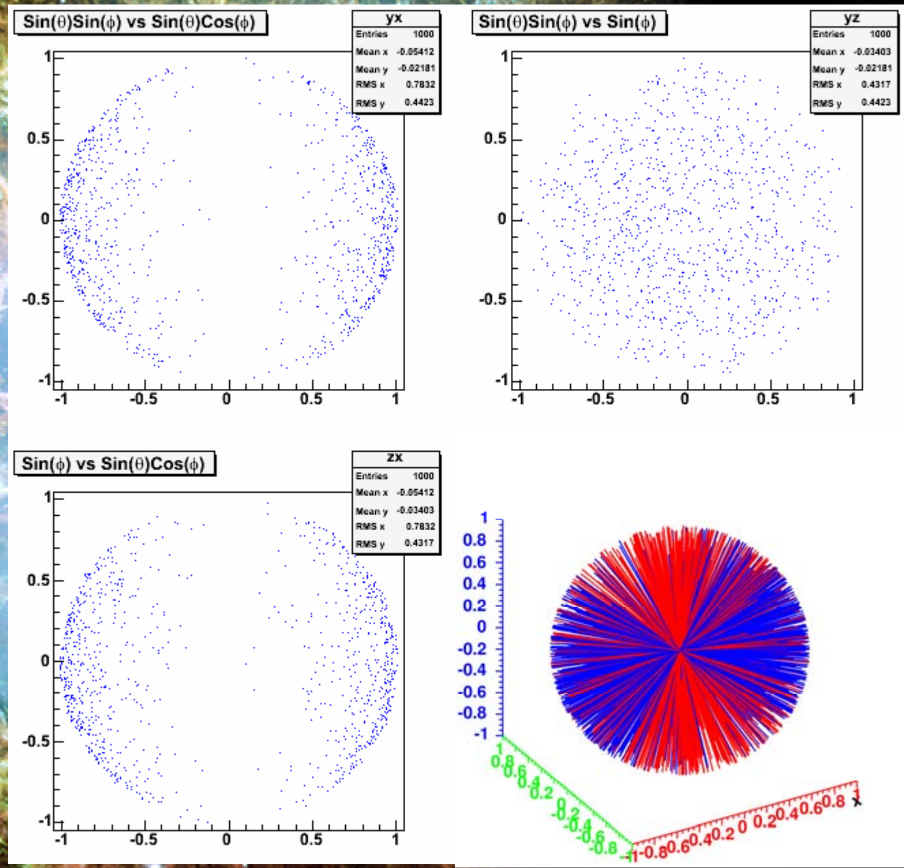


Auger emission directions

Photoelectron emission directions

# The principle of detection

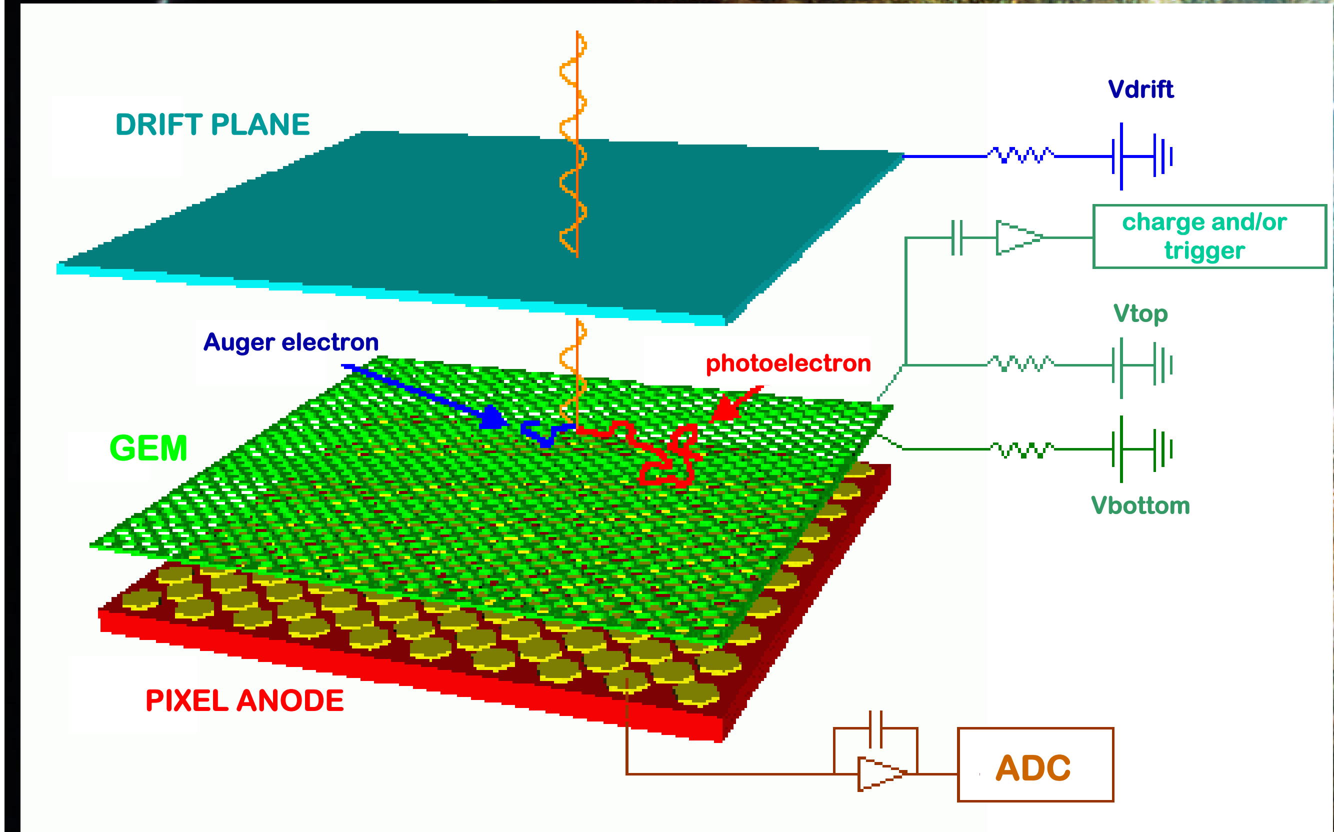


GEM electric field

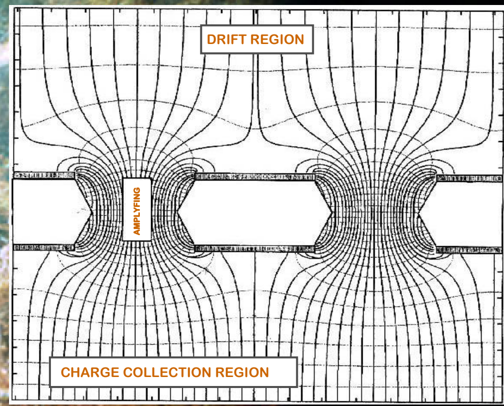


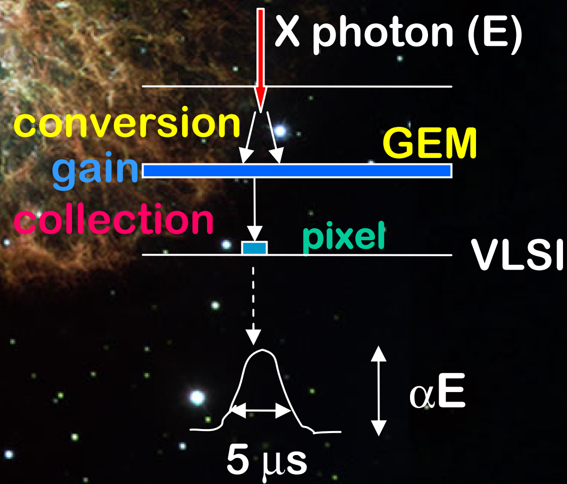


A custom CMOS analog chip is at the same time the pixelized charge collecting electrode and the amplifying, shaping and charge measuring front-end electronics of Micropattern Gas Detectors (MPGD) or other suitable charge multiplier

# Tracks reconstruction

1) The track is recorded by the PIXel Imager

2) Baricenter evaluation

3) Reconstruction of the principal axis of the track: maximization of the second moment of charge distribution

4) Reconstruction of the conversion point: major second moment (track length) + third moment along the principal axis (asymmetry of charge release)

5) Reconstruction of emission direction: pixels are weighted according to the distance from conversion point.

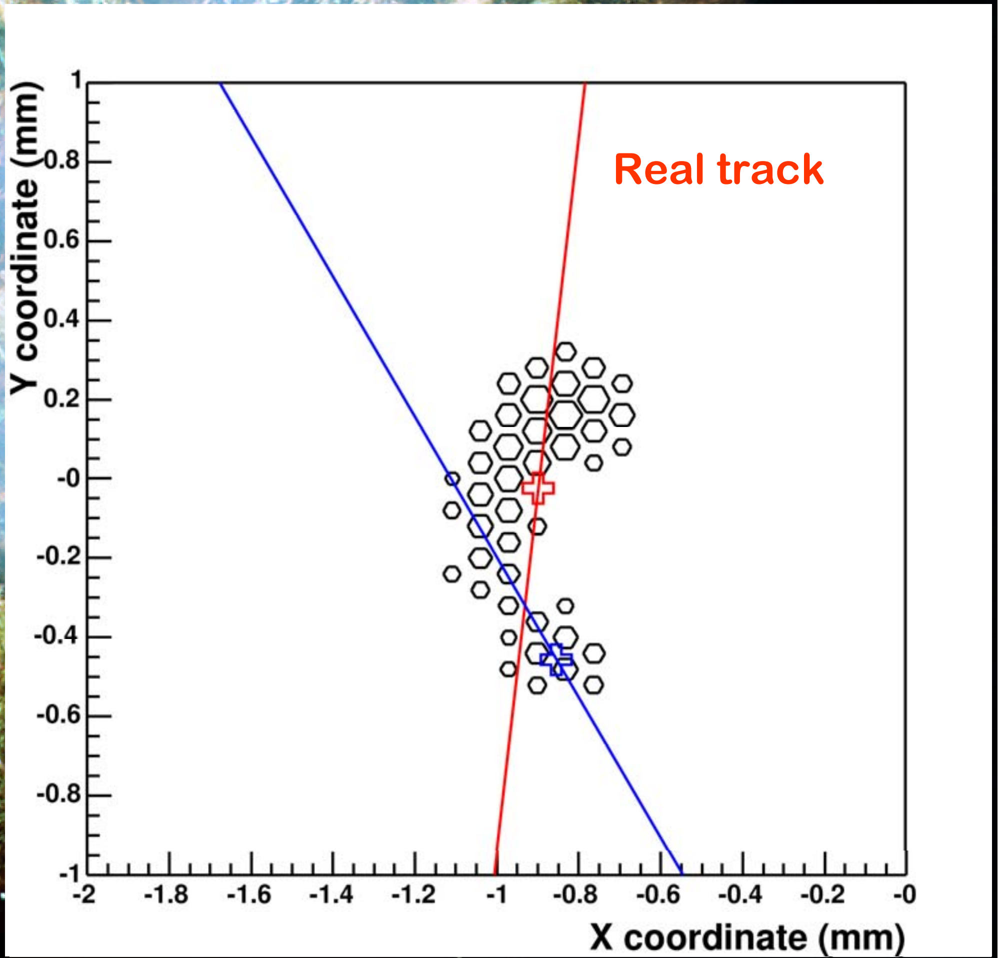

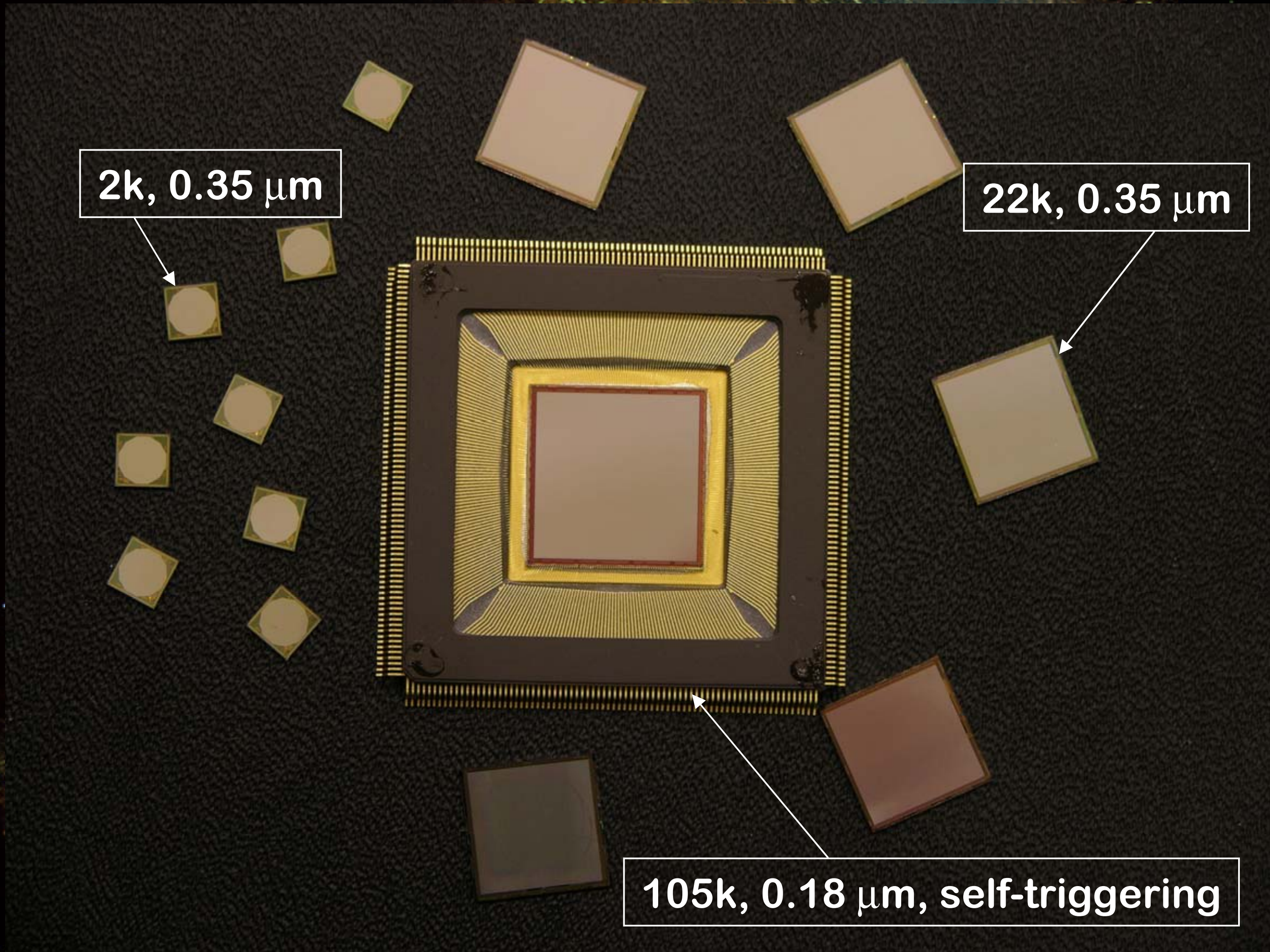


**three ASIC generations of increasing size, reduced pitch and improved functionality have been realized**

# The collecting anode/read-out VLSI chip

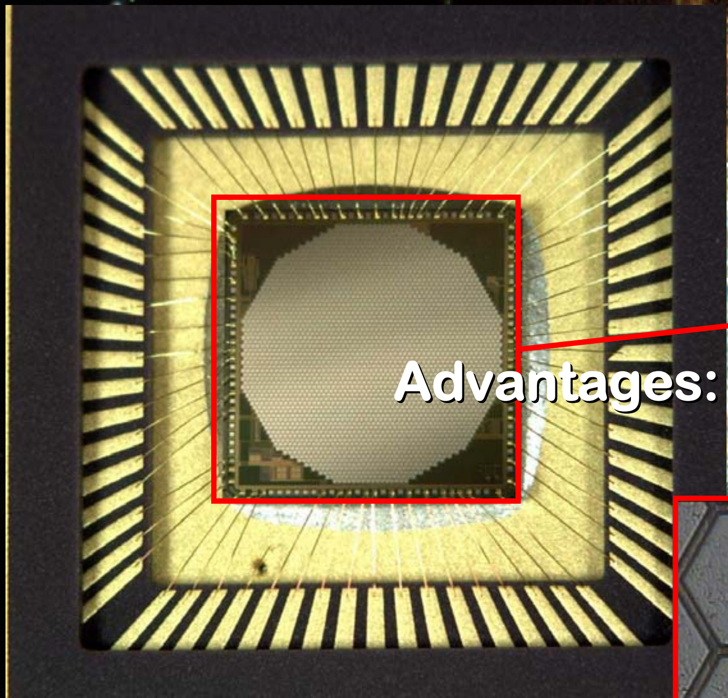

First ASIC prototype

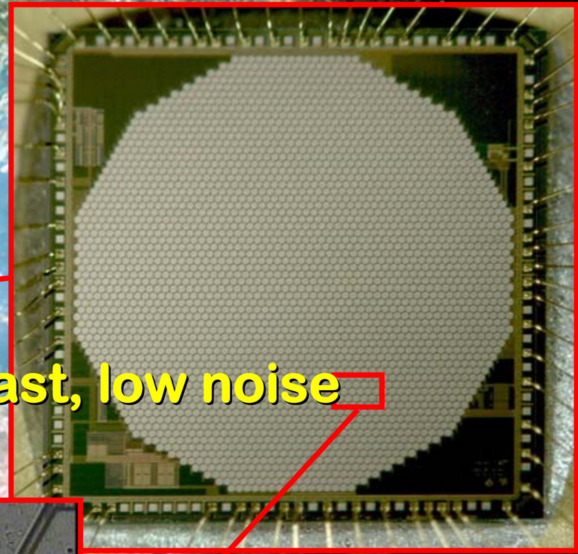

Advantages: asynchronous, fast, low noise

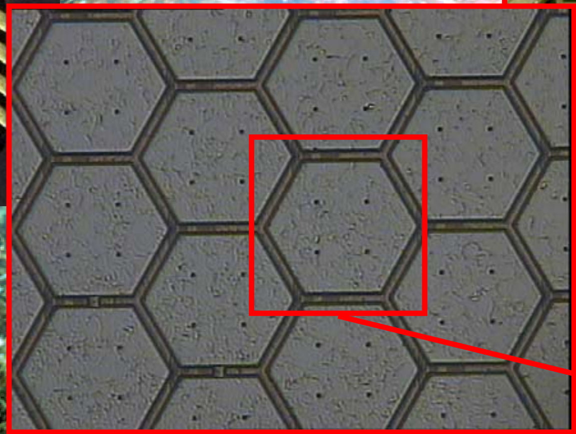

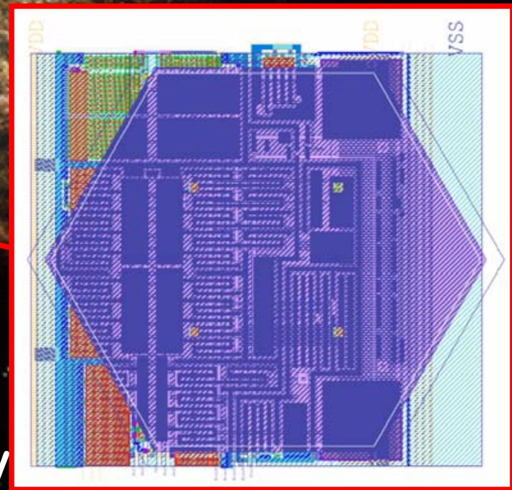

pixel electronics dimension:
80 μm x 80 μm in an hexagonal array,
comprehensive of preamplifier/shaper, S/H and routing (serial read-out) for each pixel
number of pixels: 2101

~3.5 μs shaping time
100 e- ENC
100 mv/fC input sensitivity
20 fC dynamic range

# From 2k to 22k pixels

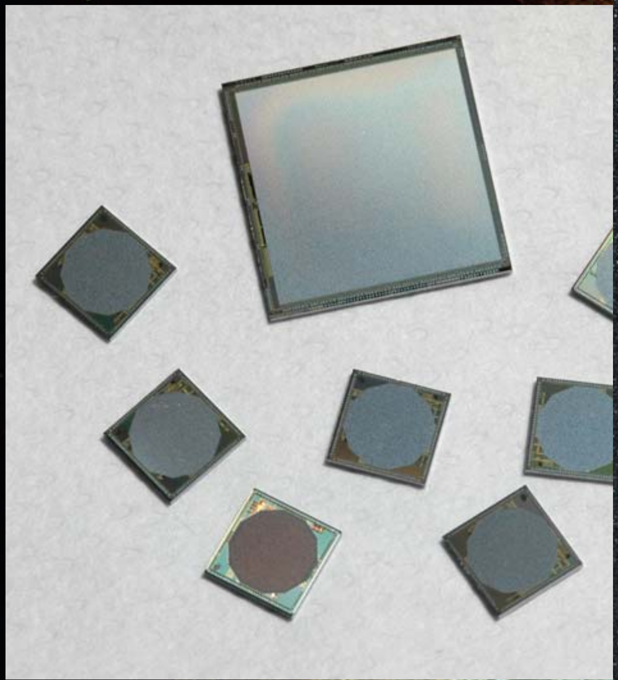

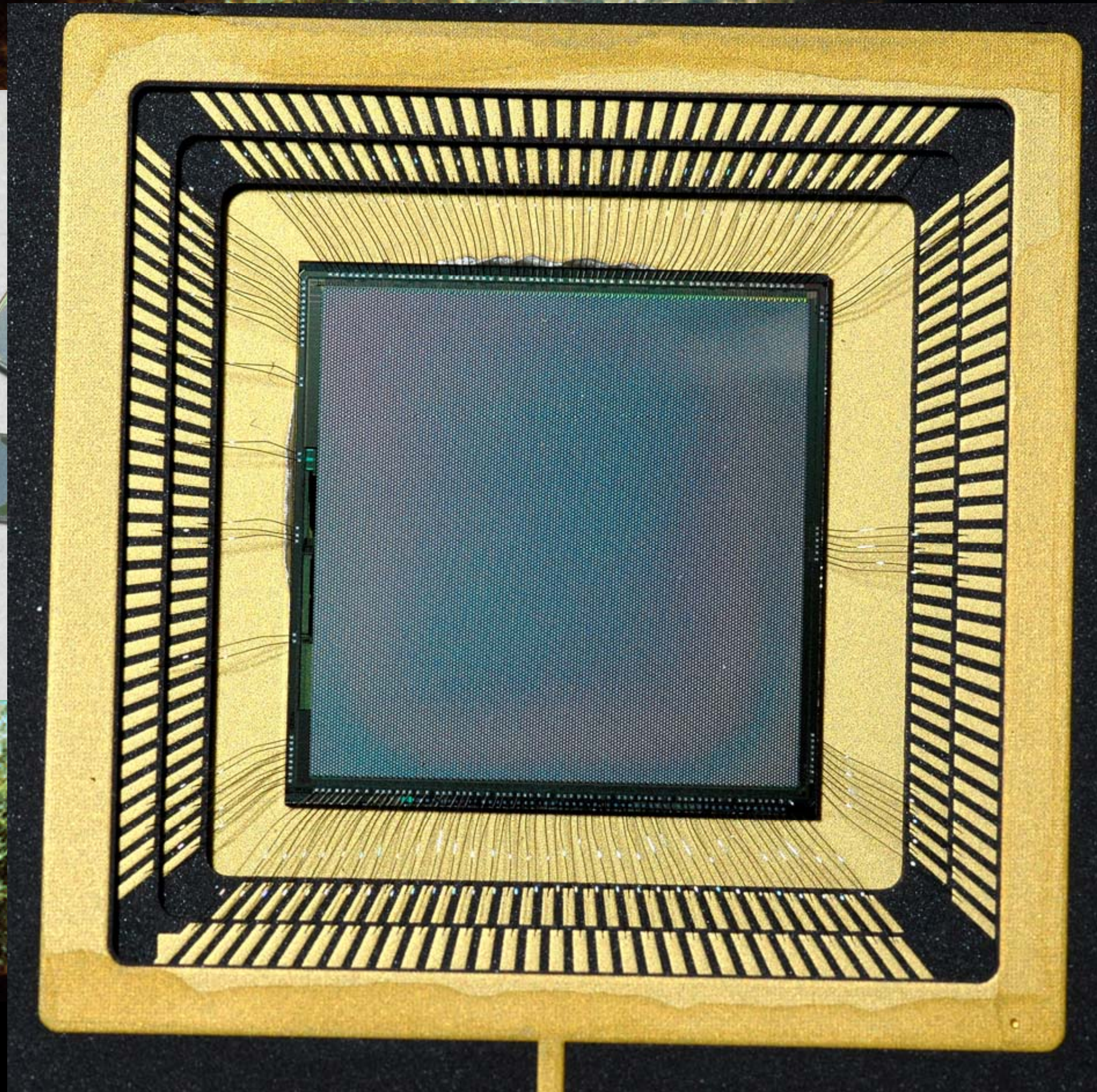

# Further technological step: a 0.18 $\mu$m CMOS VLSI

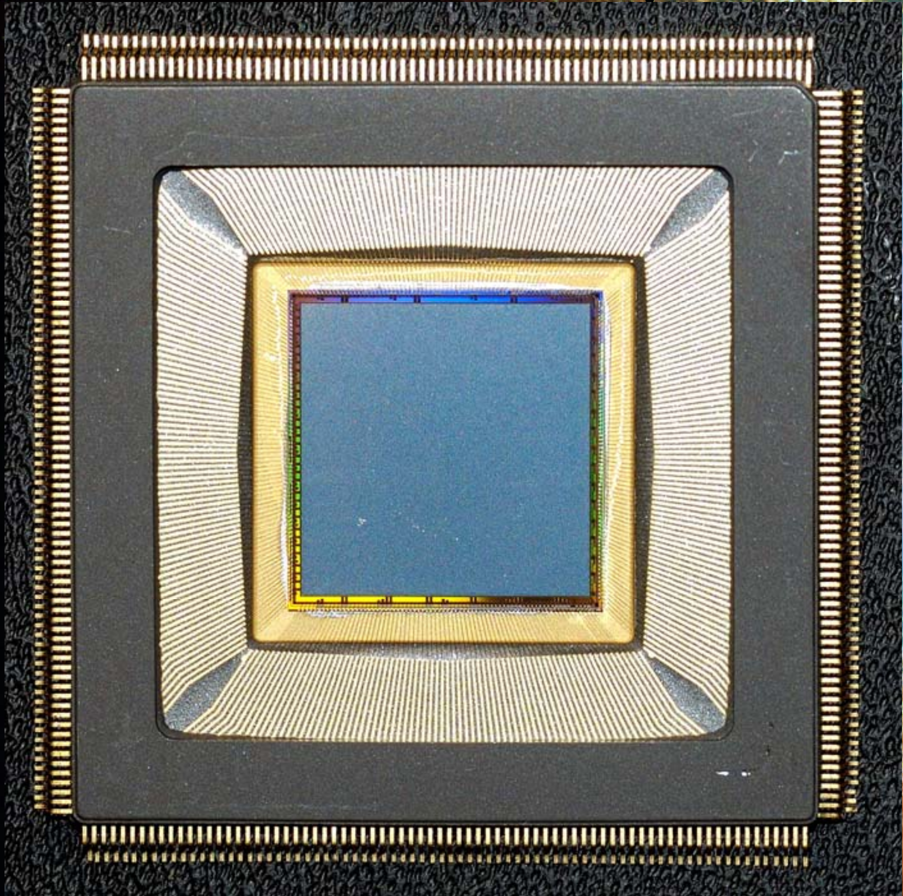

The chip integrates more than **16.5 million** transistors.
It has a **15mm x 15mm** active area of **105'600** pixels organized in a honeycomb matrix

470 pixels/mm$^2$

**Matrix organization**

300 (width=300x50$\mu$m=15mm) x 352 (height=352x43.3$\mu$m=15.24mm) pixels
16 clusters of 300 x 22 = 6600 pixels each or
8 clusters of 300 x 44 = 13200 pixels each

# 0.18 μm ASIC features

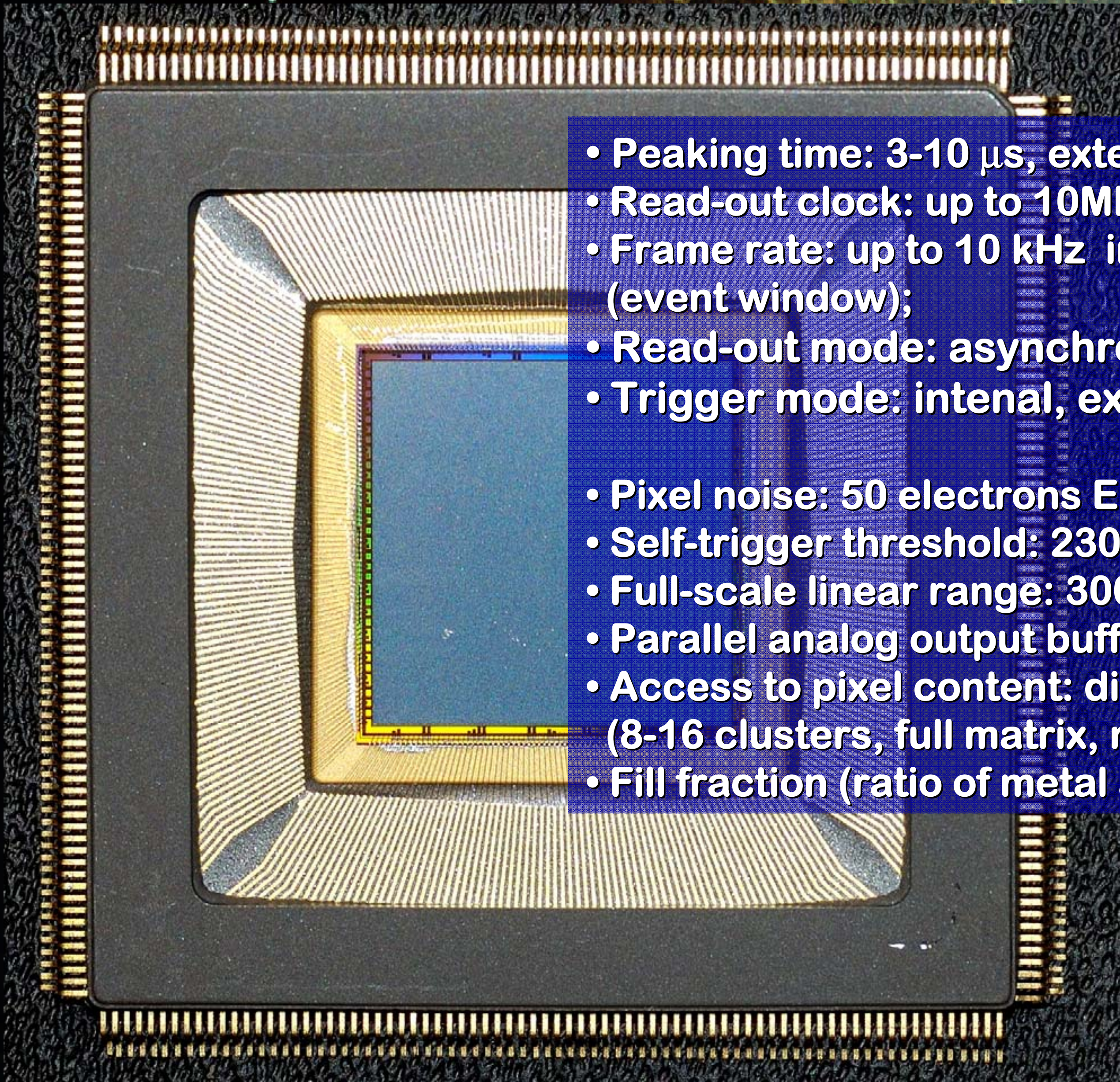

- Peaking time: 3-10 μs, externally adjustable;
- Read-out clock: up to 10MHz;
- Frame rate: up to 10 kHz in self-trigger mode (event window);
- Read-out mode: asynchronous or synchronous;
- Trigger mode: intenal, external or self-trigger;

- Pixel noise: 50 electrons ENC;
- Self-trigger threshold: 2300 electrons;
- Full-scale linear range: 30000 electrons;
- Parallel analog output buffers: 1, 8 or 16;
- Access to pixel content: direct (single pixel) or serial (8-16 clusters, full matrix, region of interest);
- Fill fraction (ratio of metal area to active area): 92%

**Total power dissipation ~ 1Watt**

# Self-trigger functionality

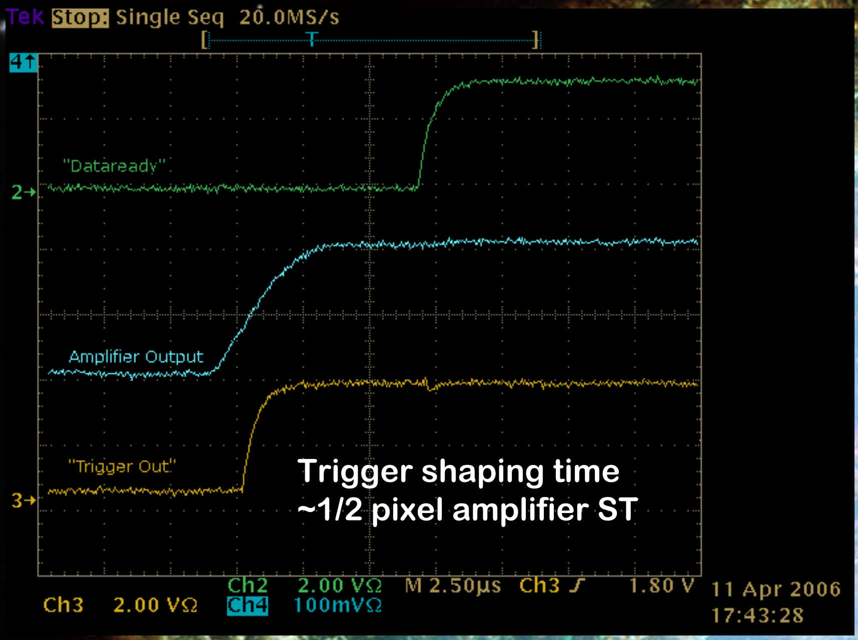


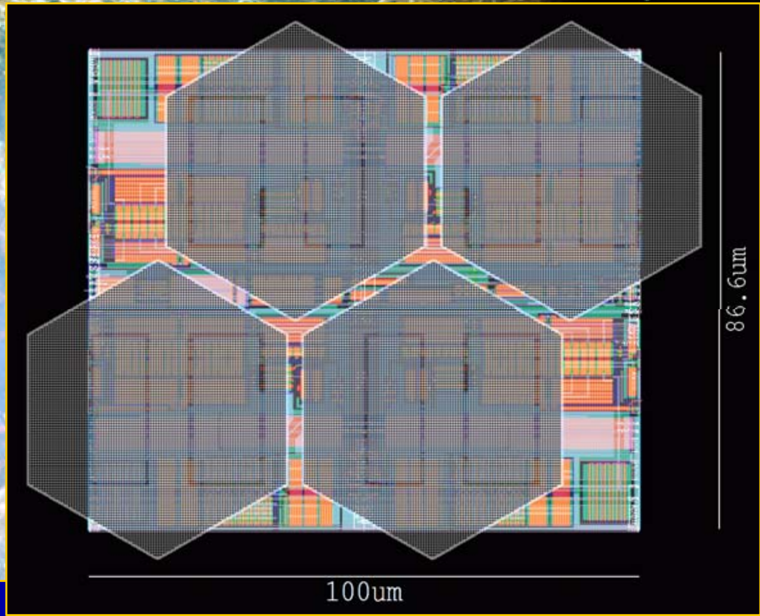


- ✓ charge sum of mini-cluster of 4 pixels contribute to a <u>local</u> trigger with dedicated s.a.
- ✓ threshold < 3000 $e^-$ (10% FS)
- ✓ individual pixel trigger mask
- ✓ independent trigger level for each 16 clusters
- ✓ event localization in rectangle containing all triggered mini-clusters + user selectable region of 10 or 20 pixels
- ✓ the chip calculates the event ROI ($X_{min}$,$Y_{min}$ – $X_{max}$,$Y_{max}$) for subsequent sequential readout of selected area

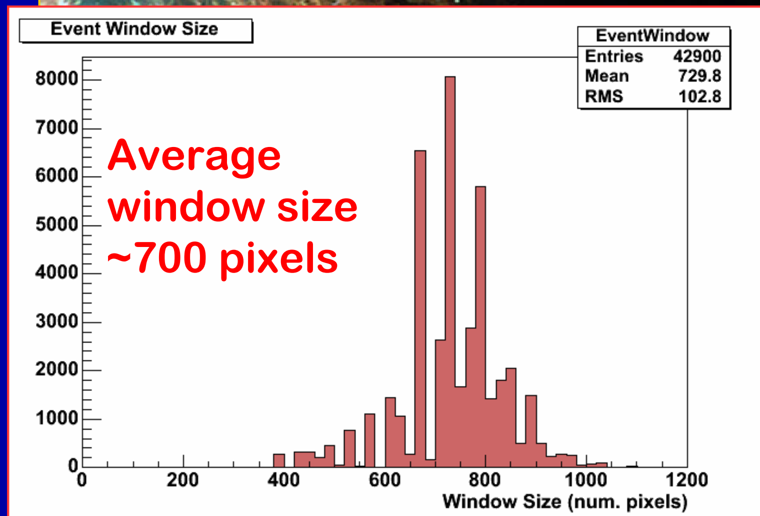

# Noise and threshold

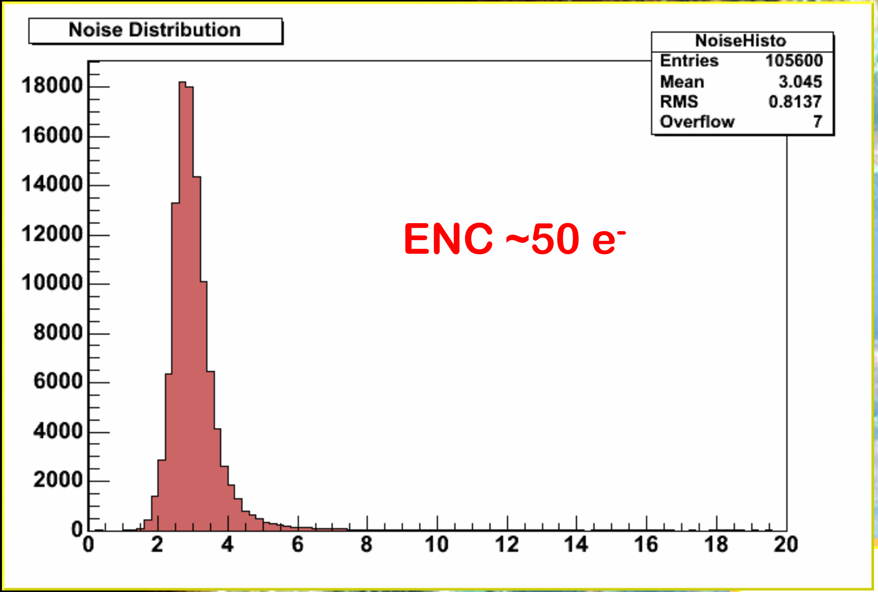


**Self-trigger threshold constrained by pedestal offset more than pedestal fluctuations**

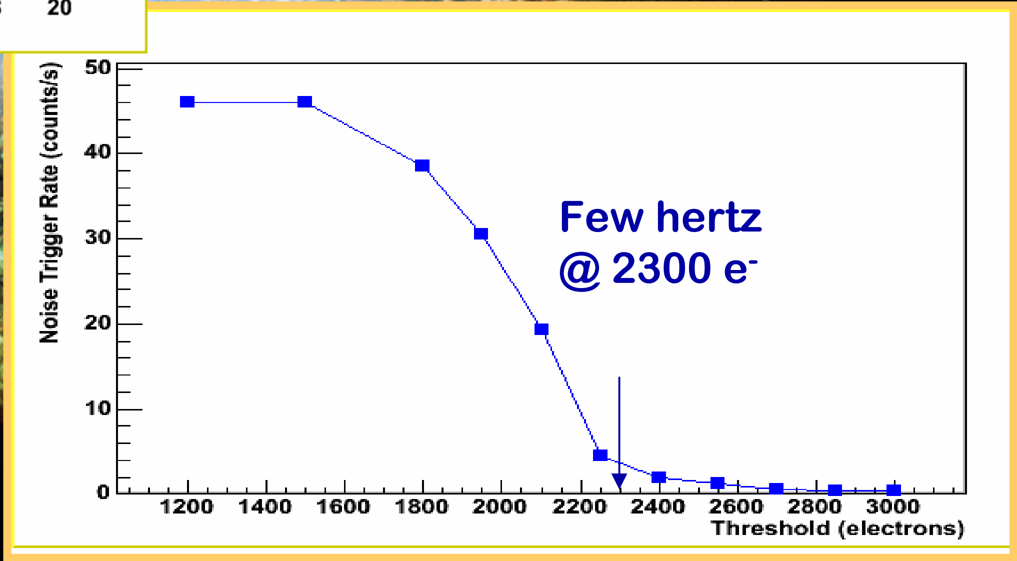

# Detector assembly

- GEM pitch: 50 μm
- GEM holes diameters: 33 μm, 15 μm
- Read out pitch: 50 μm
- Absorption gap thickness: 10 mm
- Collection gap thickness: 1 mm

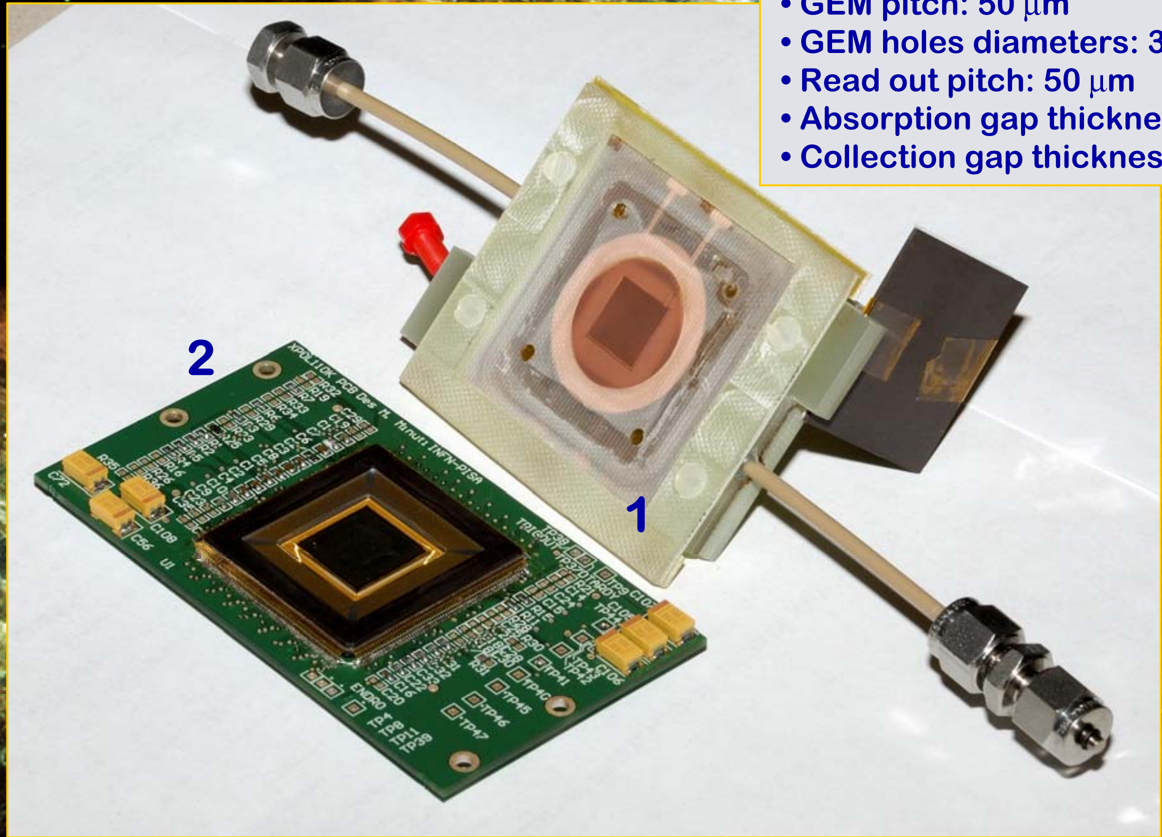


**1 - The GEM glued to the bottom of the gas-tight enclosure**
**2 - The large area ASIC mounted on the control motherboard**

**Large effective gas gain around 1000 @450V in Ne(50%)-DME(50%) (at least 70 V less than in our standard 90 μm pitch GEM)**

# GEM specs

pitch: 50 μm

holes outer Ø: 35 μm

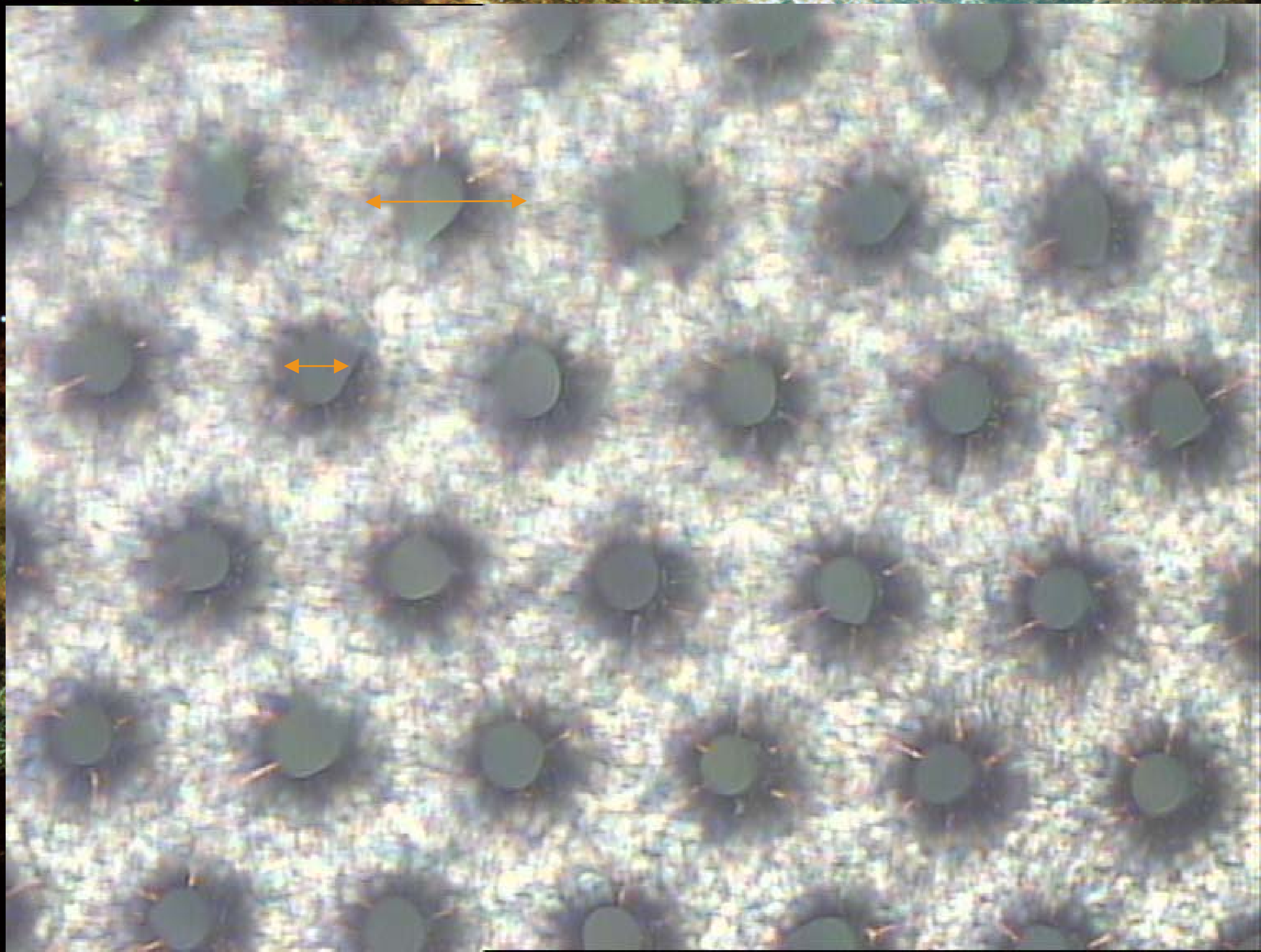

**The matching of readout and gas amplification (GEM) pitch allows getting optimal results and to fully exploit the very high granularity of the device**

# The read-out system

# On-line monitoring

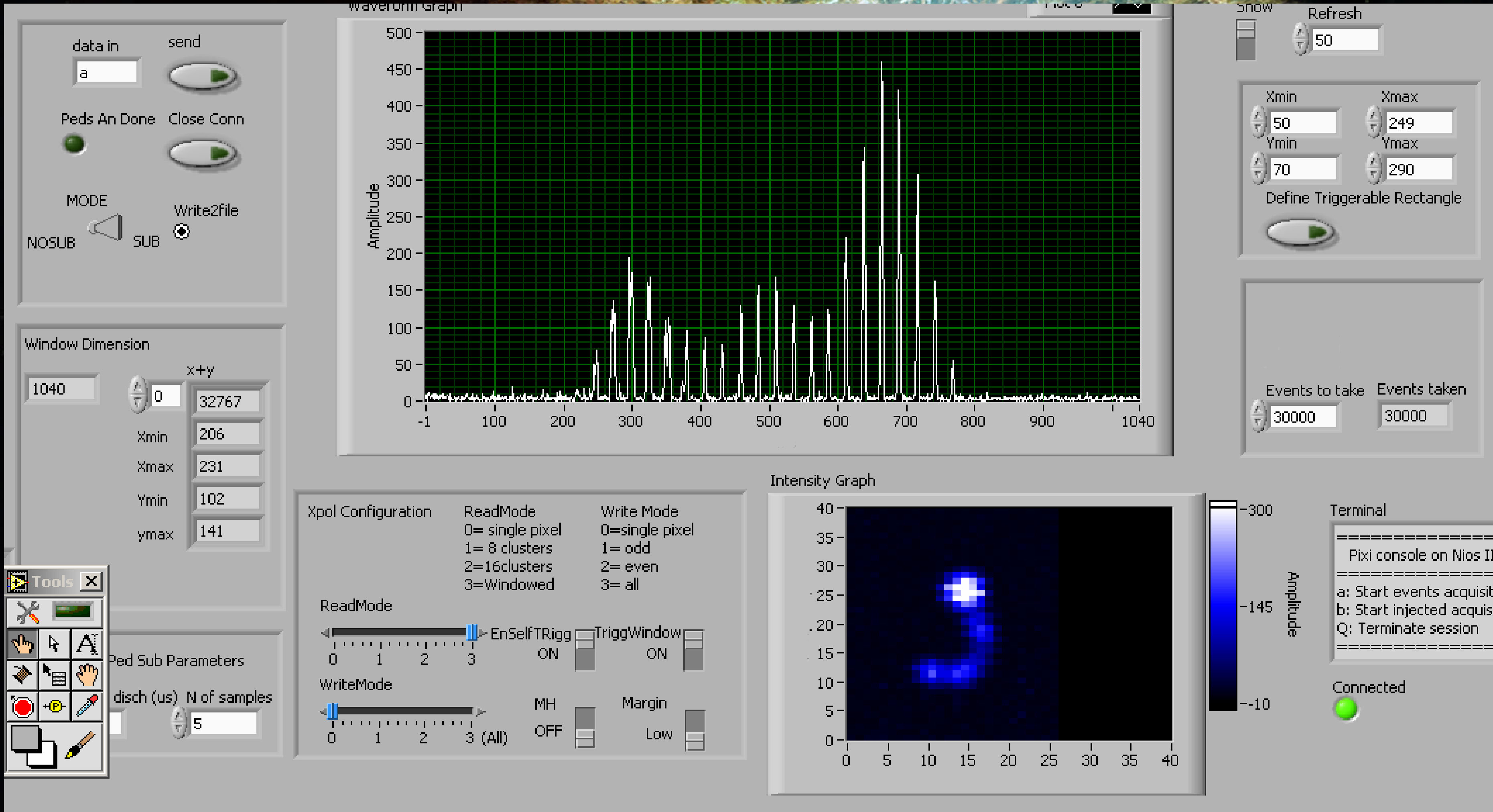


Real time pedestal subtraction

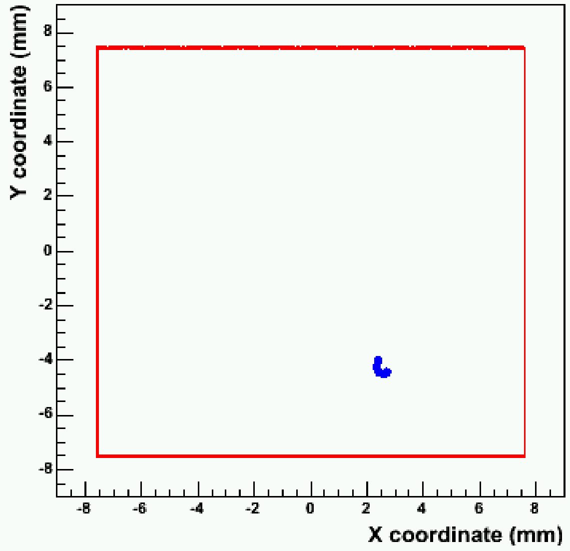


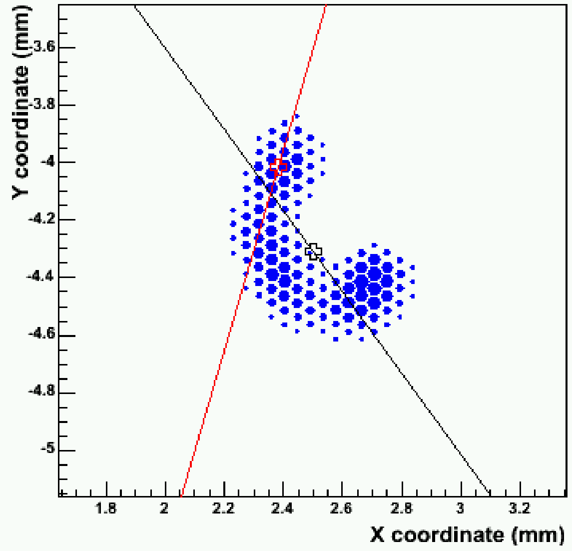


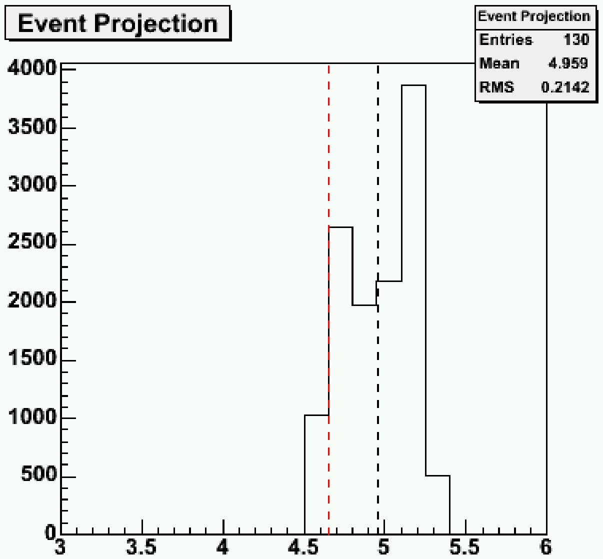


| | |
|---|---|
| Event Number: | 101 |
| Number of Clusters: | 1 |
| Cluster Size (largest): | 130 |
| Pulse Height: | 12208.2 |
| Signal to Noise: | 320.1 |
| Baricenter: | 2.50 -4.31 |
| Conversion Point: | 2.38 -4.01 |
| Second Mom Max: | 0.0459 |
| Second Mom Min: | 0.0134 |
| Shape (ratio of moments): | 3.42 |
| Third Mom Max: | -2.6e-03 |
| Phi (iteration 1) | -0.9540 |
| Phi (iteration 2) | -1.8518 |

Reconstructed Baricenter

Reconstructed Impact Pt.

# Imaging capability

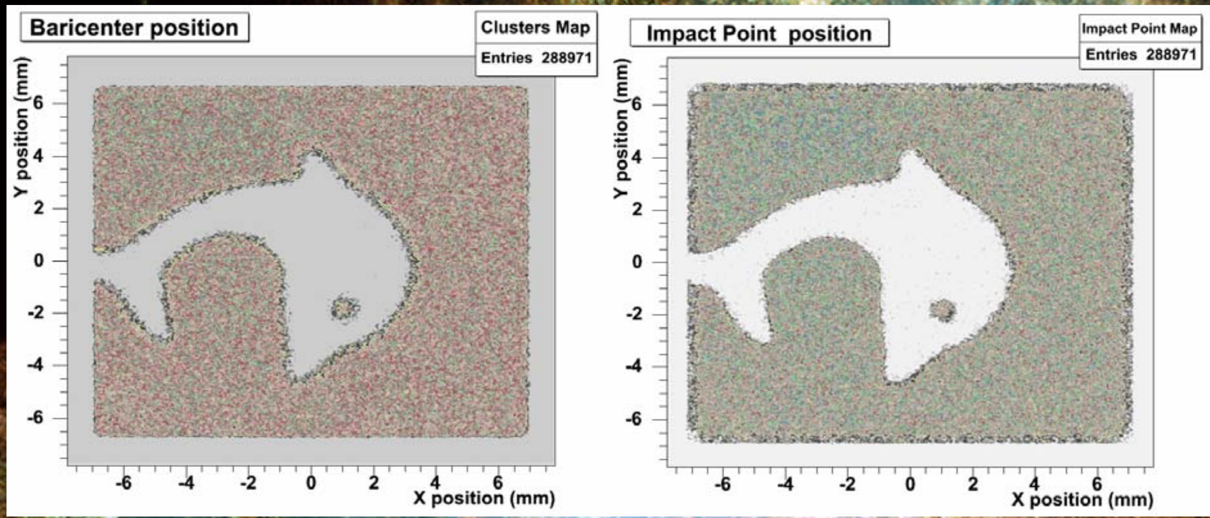


$^{55}$Fe source **Ne(50%)-DME(50%)**

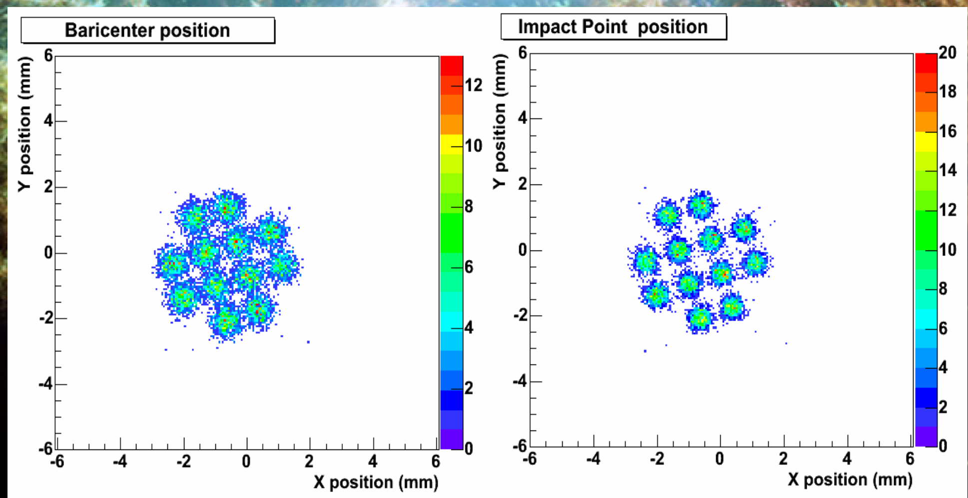


**Holes: 0.6 mm diameter, 2 mm apart.**

# Imaging and spectroscopic capability

Argon (50%)-DME(50%)

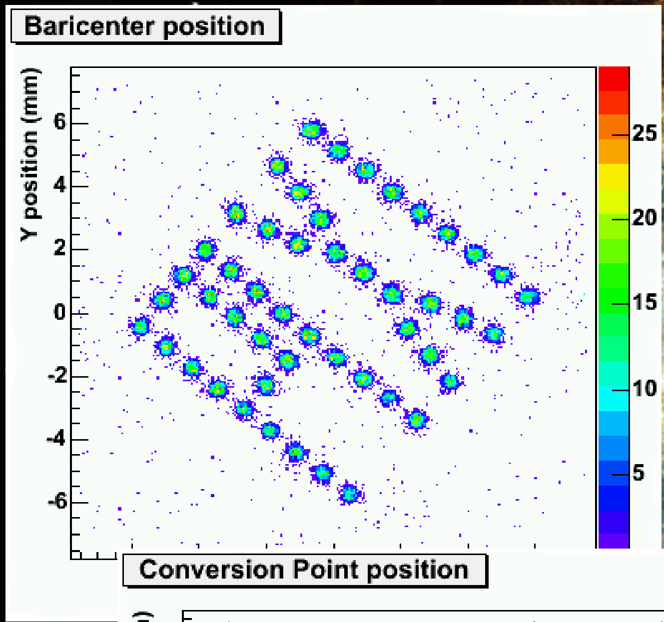


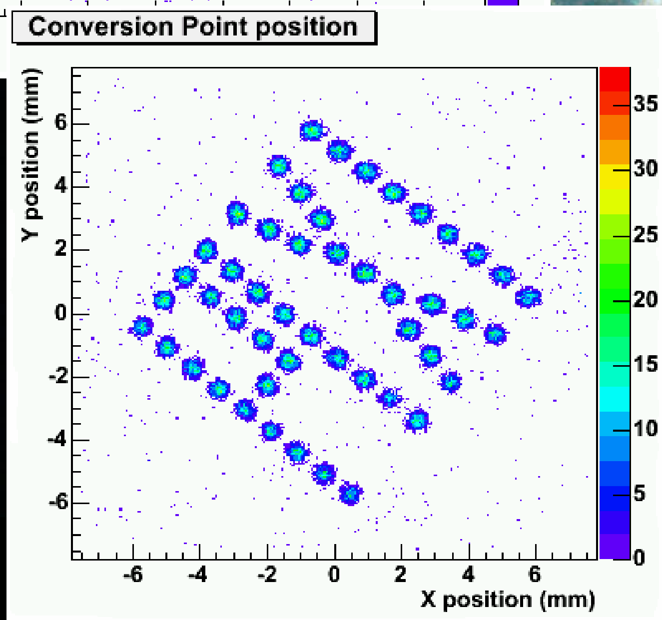


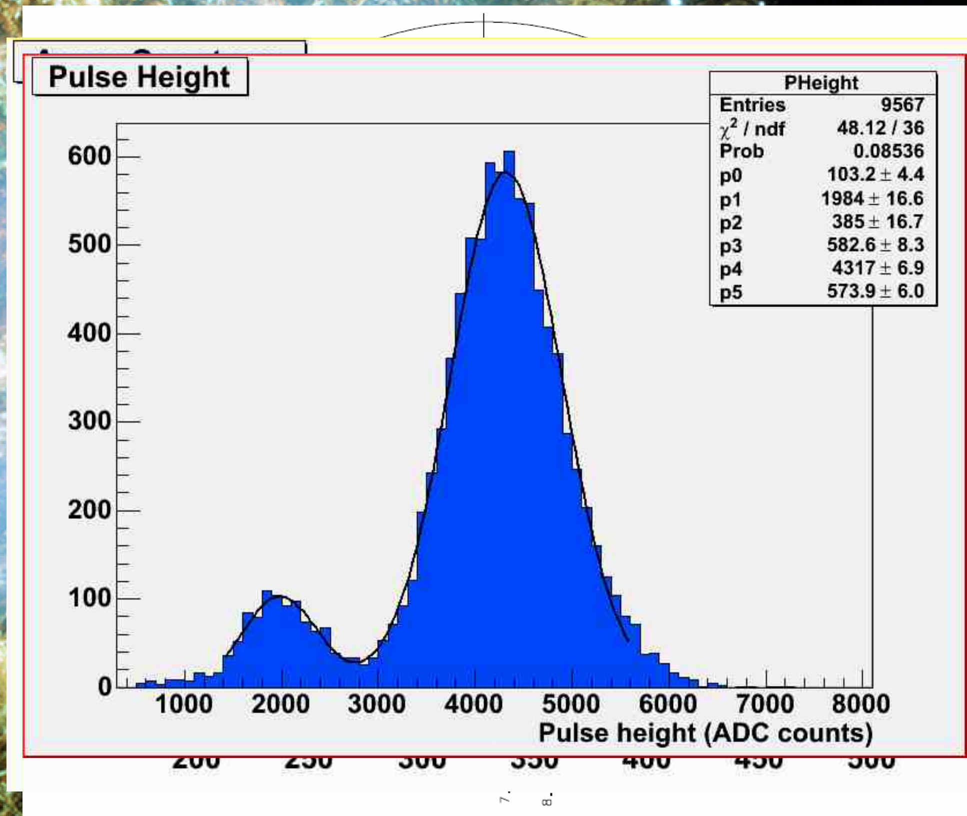


Holes:
Ø 0.5 mm
pitch 1 mm

# Polarizing X-rays

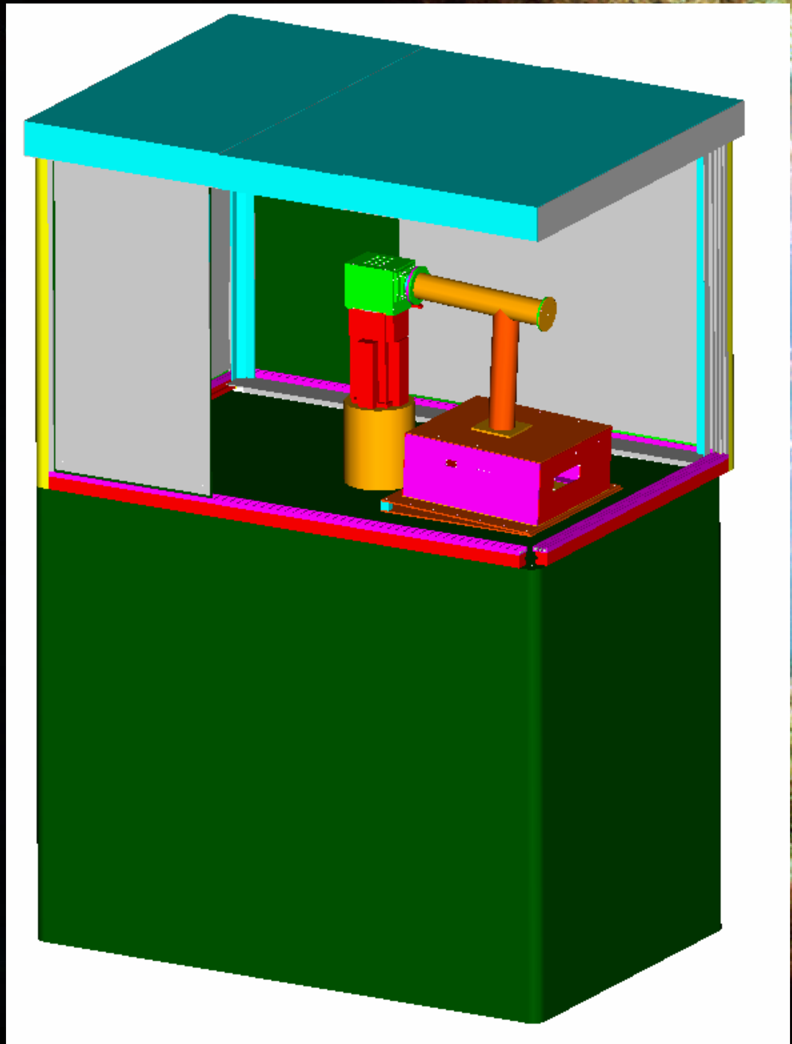

90° Thompson scattering

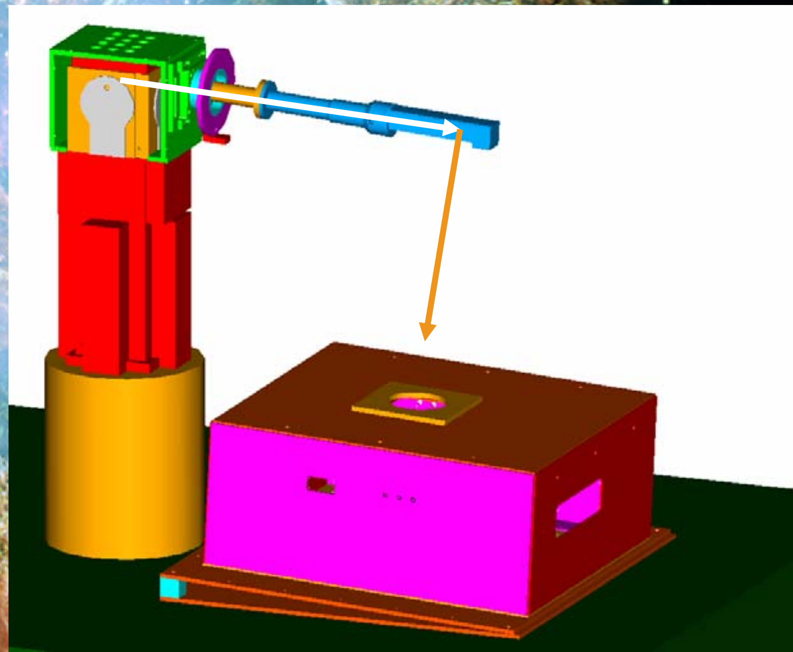

# Track morphology and angle reconstruction

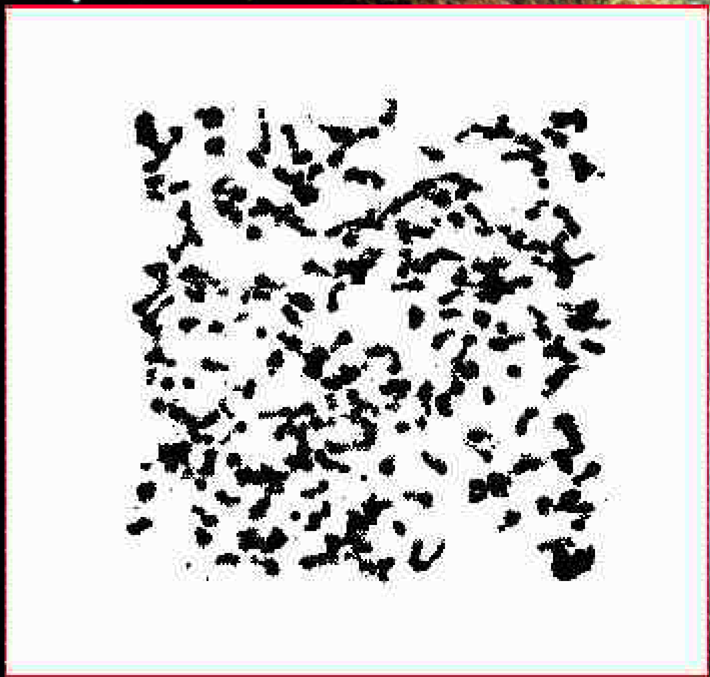

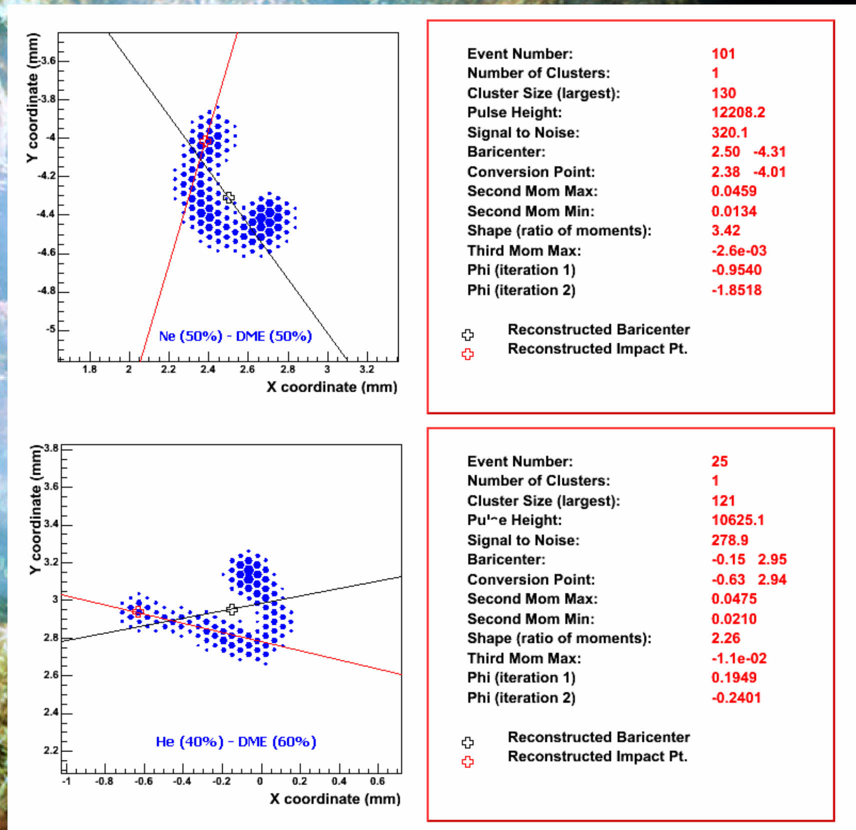

# Modulation factor

Measured with two different gas mixtures:
He/DME and Ne/DME

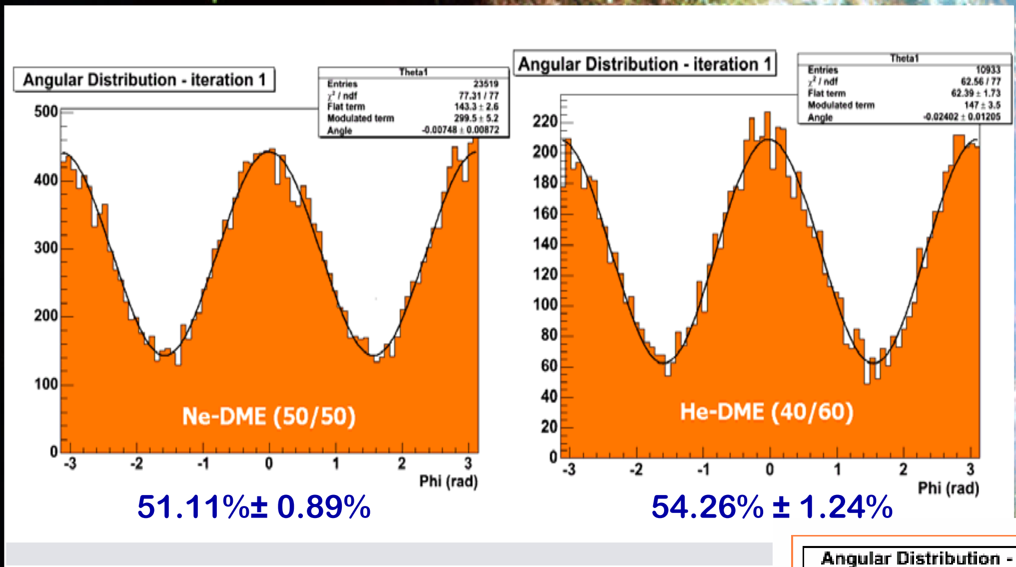


@5.4 keV Cr-line energy

@6.4 keV Fe energy

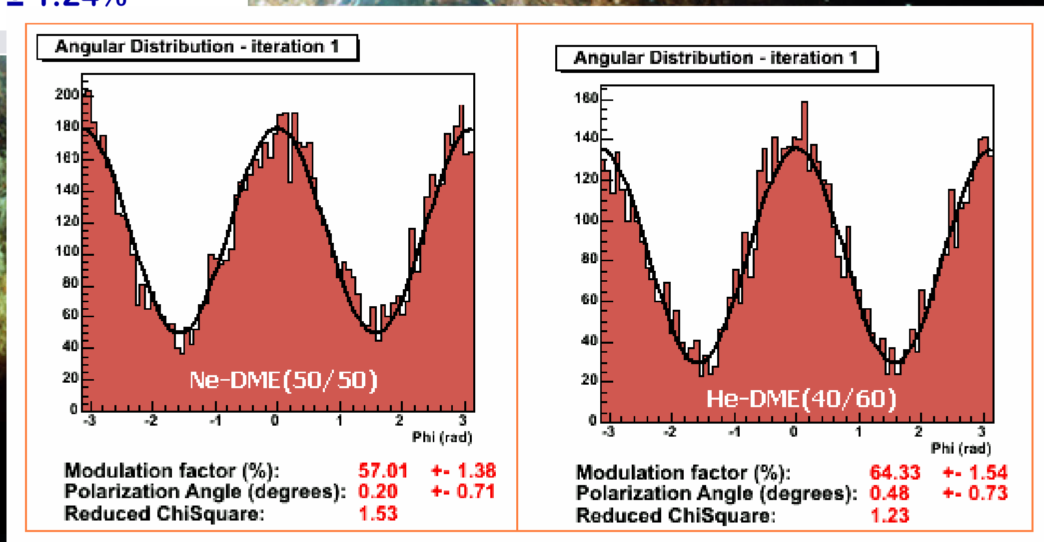

# Residual modulation

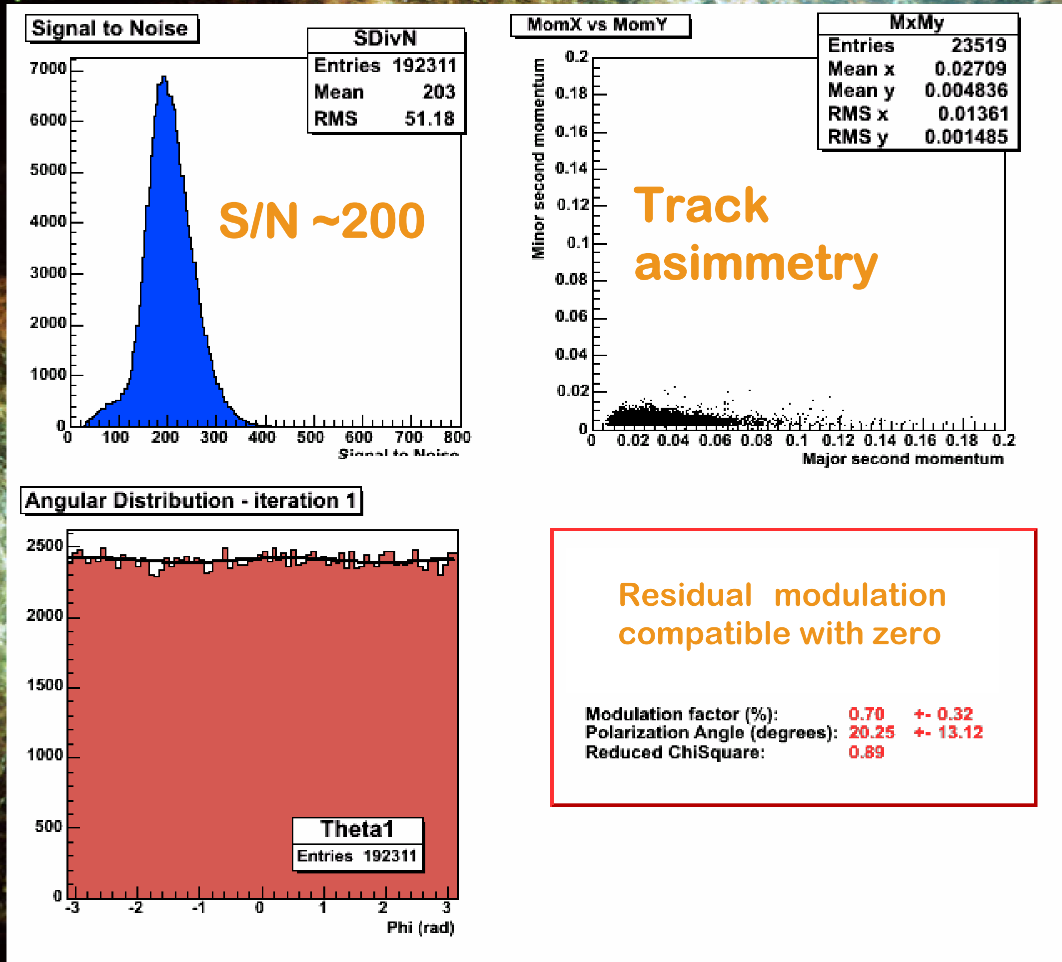


**S/N distribution, scatter plot of the two principal axes of the cluster charge and residual modulation, obtained with $^{55}Fe$ source in Ne(50%)-DME(50%)**

# MC simulation
# MDP for Crab & Her-X1

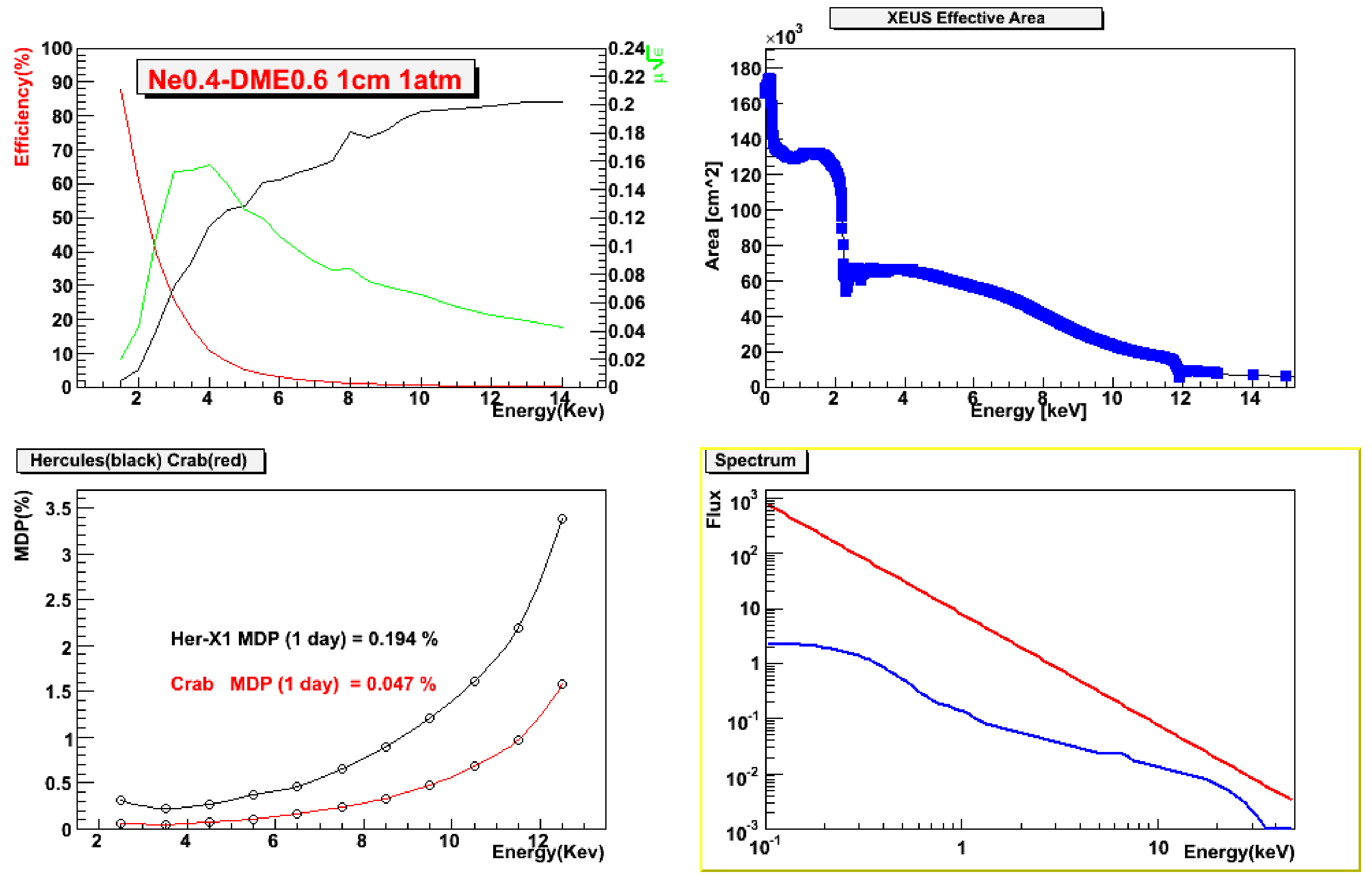


**XEUS mirror effective area is considered in simulation**

# Expected MDP with XEUS optics
## @ different source fluxes and spectral index

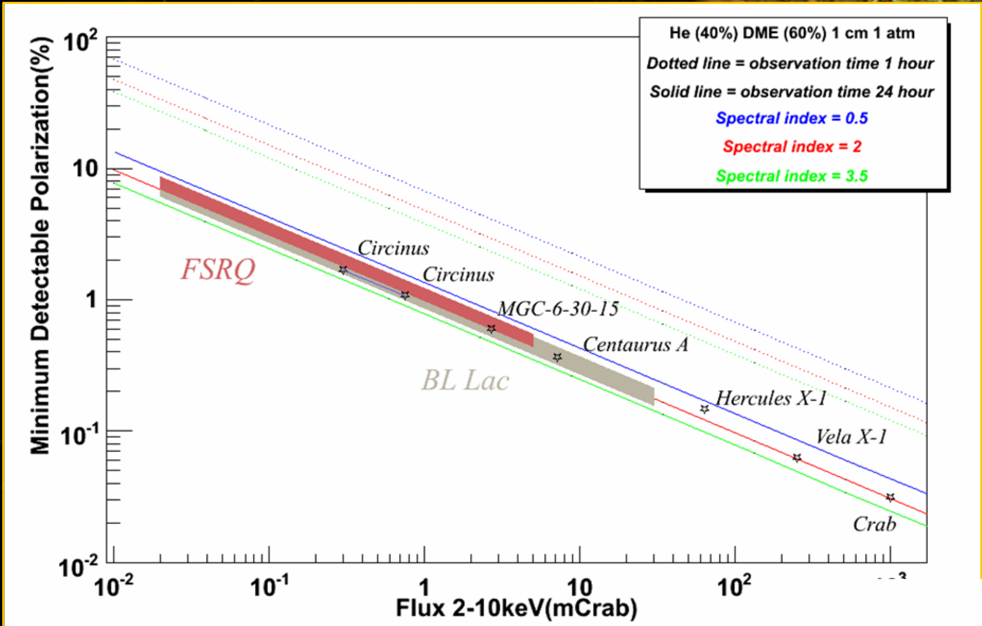


He(40%)-DME(60%)

With observations of one day we can measure the polarization of several AGNs down to 1 % for 1 mCrab flux

With 1 h it is possible to get few % with a 10 mCrab flux

Ne(50%)-DME(50%)

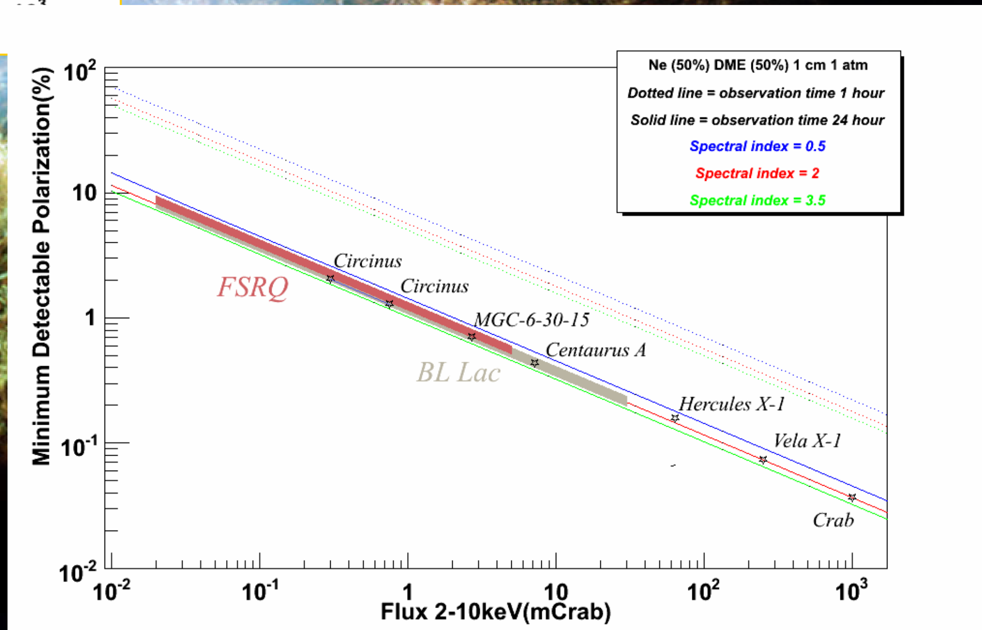

# The only polarized source already known

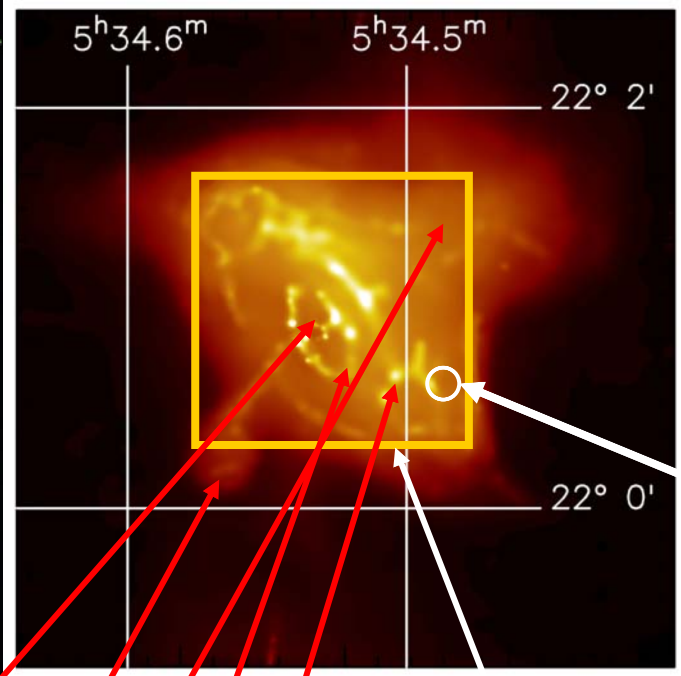


p.s.f.

f.o.v.

PSR

NW jet

SE jet

Inner torus

Outer torus

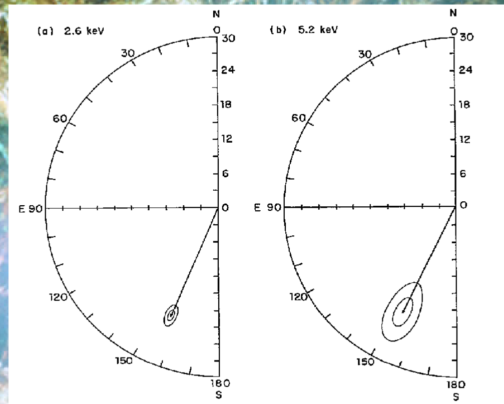


**Positive measurement: of X-ray polarization of the Crab Nebula without pulsar contamination (by lunar occultation, Weisskopf et al., 1978).**

**$P = 19.2 \pm 1.0$ %**

**$\theta = 156.4^{o} \pm 1.4^{o}$**

**But this is only the average measurement.The structure is much more complex!**

**With XPOL we can perform the separate polarimetry, imaging, spectroscopy and timing of details of the major structures**

# The resolution of the polarimeter is better than the telescope

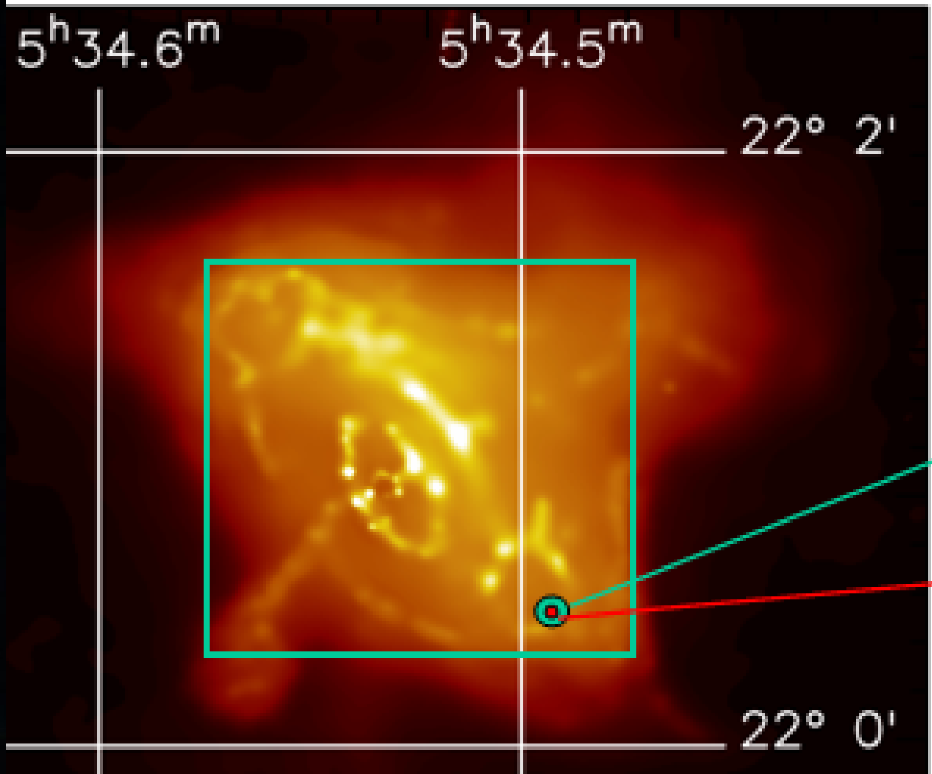


| | Angular | Linear |
|---|---|---|
| FOV | **1.5'x1.5'** | **1.5x1.5 cm** |
| PSF Telescope | 5'' | 848 **µm** |
| PSF Detector | 0.88'' | 150 $\mu$m |

# Rotation of polarization angle under GR effects

The polarization plane rotates continuously with energy because of General Relativistic effects. This is a signature of the presence of a black-hole
(Stark& Connors, Connors& Stark, 1977, Connors, Piran & Stark, 1980).

**Cygnus-X1**
**Flux: 0.78 Crab**
**Spectral index: 1.9**
**Observ. Time: 12 h**
**Polarization:5%**

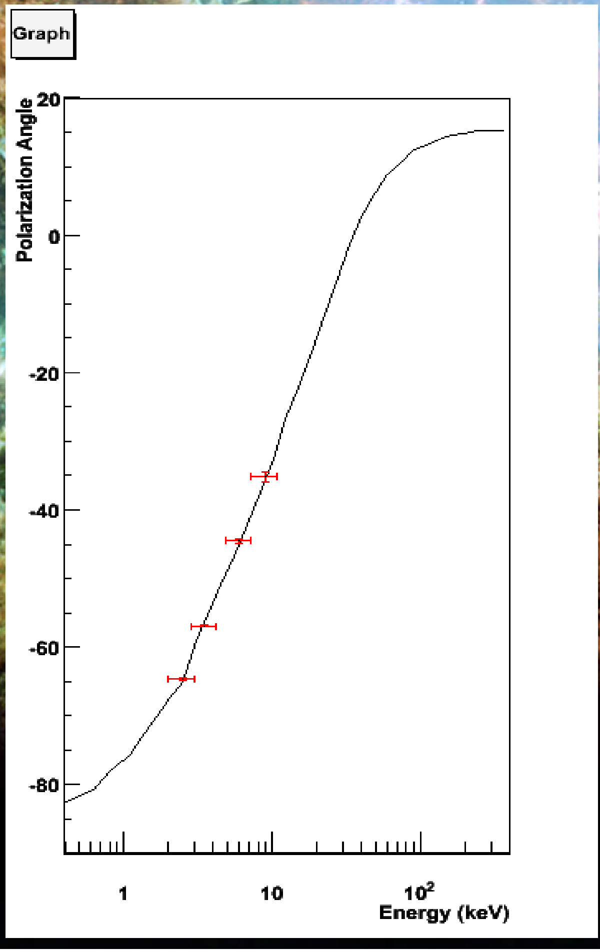


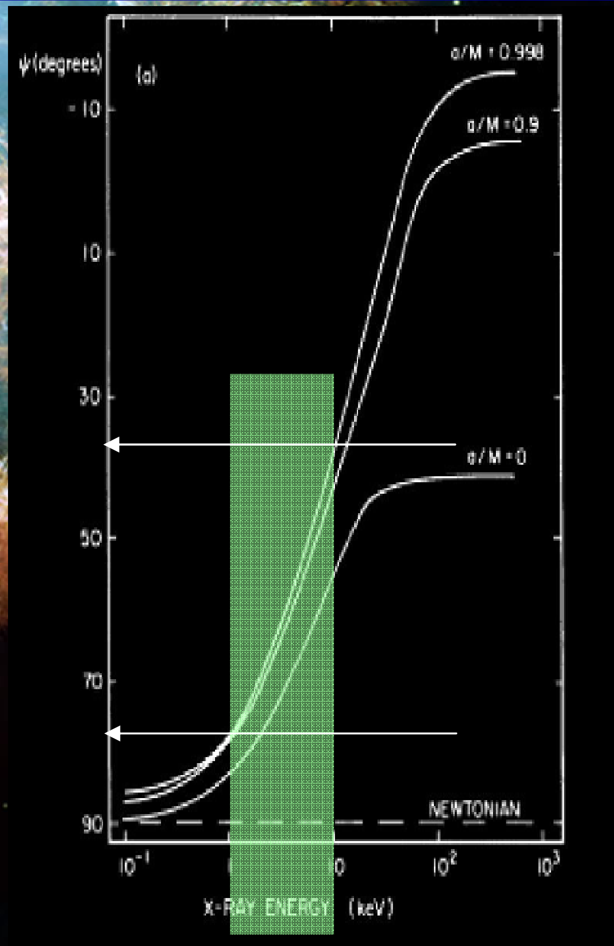

# Time variability of polarization degree and angle

## The case MCG-6-30-15

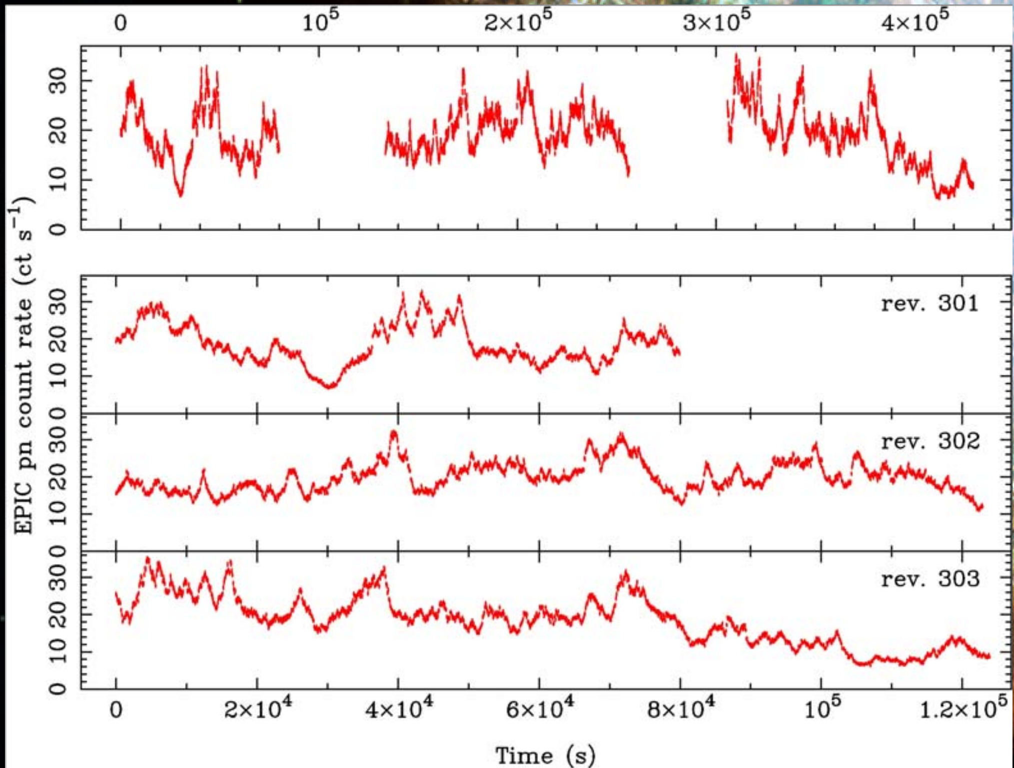


Top Three consecutive light curves. Bottom the three individual lightcurves Vaughan, Fabian Nandra (2003)

Variability of the continuum are correlated to the height of the primary source The height of the primary source implies a variation of the polarization degree and angle of the reflected radiation

Time scale for variation are $10^4$ s .

**In $10^4$ s MDP is 3 %**

The inclination is 30º for MCG-6-30-15 (Tanaka et al. 95) and for this large inclination polarization degree expected can be larger in $10^4$ s.

Observation of polarization degree variability in $10^4$ observing time can be decisive to test the model of illuminated accretion disk.

# Archeology of the Galactic Center

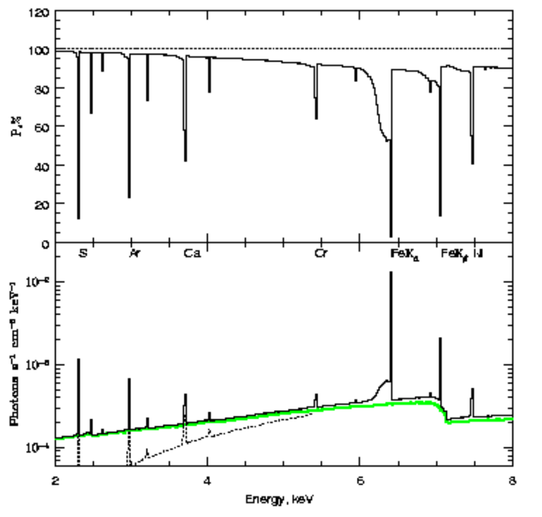


**Figure 1.** Bottom panel: A reflected energy spectrum (the solid line) of a spherical cloud exposed to hard X-ray emission from an external source. The cloud is assumed to be at the same distance from the observer as the primary source. The spectrum is shown with the energy resolution of 20 eV. The brightest fluorescent lines of the most abundant elements are marked. Note that for Ca, Cr and Ni the two components of the $K_\alpha$ lines ($K_{\alpha_1}$ and $K_{\alpha_2}$) fell into adjacent energy bins causing the lines to look broader. The dotted line shows the suppression of the low energy part of the spectrum due to a photoabsorption over the line of sight for the hydrogen column density of 5 $10^{22}$ $cm^{-2}$. The grey line shows the Stokes Q parameter, defined relative to the direction from Sgr A* to Sgr B2, as a function of energy (the U parameter is equal to zero). Top panel: Degree of polarization in the reflected spectrum. In the simulated geometry an average scattering angle of the primary radiation is close to 90°and the continuum radiation is almost completely polarized. The degree of continuum polarization slowly decreases with energy due to the increasing contribution from multiple scatterings. The fluorescent lines are produced in the cloud itself and are emitted isotropically. As a result degree of polarization drops strongly at the energies of the lines.

(Churazov, E, Sunyaev, R, Sazonov, S. MNRAS, 330 no.4 817 2002)

- In the Galactic Center there is a BH of $2.6 \times 10^6$ $M_o$
- Now is QUIET, but some hundreds years ago was BRIGHT!

(Galileo and Brahe would have probably observed the GC as the brightest extrasolar X-Ray source!)

- Sgr B2 is a molecular cloud ~ 100 pc from the GC
- In X-Ray is a pure reflector ! *(hard spectrum, fluorescent 6.4 keV line, brighter on the side of Sgr A*)*
- The reflected flux should be HIGHLY polarized!
- Sgr B2 is echoing the PAST activity of our Galactic Center!
- X-ray polarimetric studies would allow to reconstruct real 3-dimensional positions of the scattering clouds.

# XPOL: a realistic implementation for XEUS

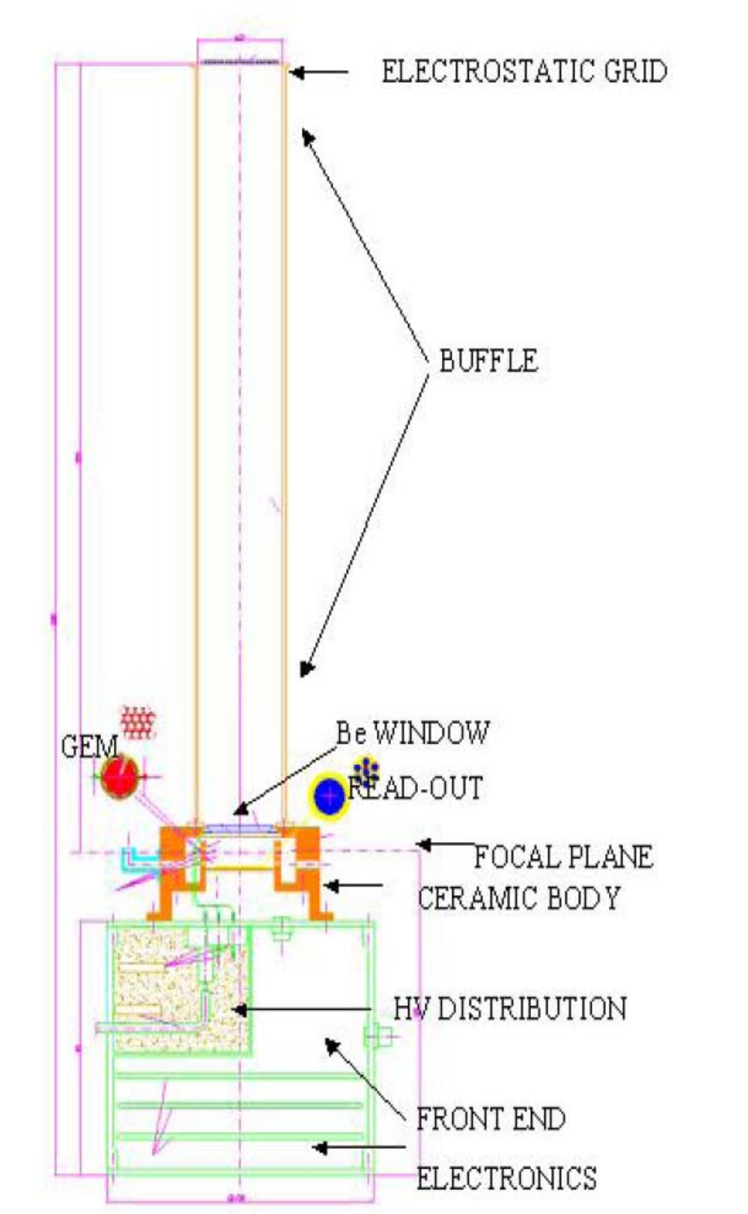


* critical parts (GEM and VLSI) do **exist**
* body, window, gas handling, HV etc. are well established technology
* relatively **small** and compact
* no cryogenics
* no rotations
* VLSI is radiation hard
* very **fast,** up tp $10^5$ c/s
* also performs **timing, imaging, spectra**

A possible design based on established technology (BeppoSAX MECS)

# Resources for XPOL

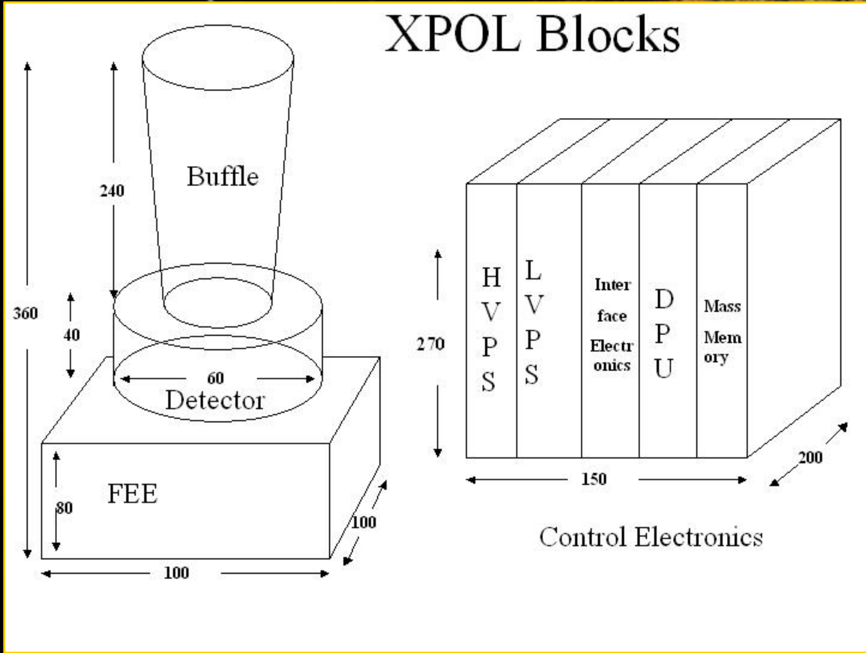


| Unit | Location from FP (cm) | Mass (kg) | Power (W) | Dimension (cm) |
|---|---|---|---|---|
| Detector+buffle | FP (ext 25 cm front 11cm back) | 2.0 | 3.5 | 28 x 6 Ø |
| FEE | | 1.5 | 3.5 | 10x8x10 |
| CE | <200 | 7.5 | 10.0 | 27x15x20 |
| Total | | 11.0 | 17.0 | 10x8x10 |

| GEM | | ASIC CHIP | | | | |
|---|---|---|---|---|---|---|
| For each photon: | | | | | | TOT |
| Time bit | Energy bit | Absorption point bit | | Emission angle bit ** | Quality parameter bit | |
| | | Coord. X | Coord. y | | | |
| 18 | 8 | 9 | 9 | 10 | 8 | 62 |

** with a statistic of 20000 events.

Data rate

# Conclusions

With the presented device the class of Gas Pixel Detectors has reached the level of integration, compactness and resolving power typical of solid state detectors.

A residual modulation very low and a modulation factor well above 50% will likely allow polarimetric measurements at the level of ~1% for hundreds of galactic and extragalactic sources.

***A real breakthrough in X-ray astronomy***
**if compared with the traditional X-ray polarimeters sensitivity.**